Studies on potential role of nonneutralizing IgA antibodies in cross-protective immunity against influenza A viruses

(A 型インフルエンザウイルスに対する交差感染防御における非中和 IgA 抗体の役割に関する研究)

Kosuke OKUYA

Contents

Abbreviations

5'-RACE	5'-rapid amplification of cDNA ends
Ad2	A/Adachi/2/1957 (H2N2)
Aichi	A/Aichi/2/1968 (H3N2)
Alb60	A/duck/Alberta/60/1976 (H12N5)
ANOVA	one-way analysis of variance
BN-PAGE	blue native polyacrylamide gel electrophoresis
BSA	bovine serum albumin
cDNA	complementary deoxyribonucleic acid
cHA	chimeric HA
ch-rM2ss23	chimeric rM2ss23
CZC	Research Center for Zoonosis Control
d-IgA	dimeric immunoglobulin A
DMEM	Dulbecco's modified Eagle's medium
ELISA	enzyme-linked immunosorbent assay
ELLA	enzyme-linked lectin assay
Eng1	A/duck/England/1/1956 (H11N6)
FBS	fetal bovine serum
GFC	gel filtration chromatography
HA	hemagglutinin
HEK	human embryonic kidney
HK483	A/Hong Kong/483/1997 (H5N1)
HRP	horseradish peroxidase
HU	Hokkaido University
IAV	influenza A virus
IgA	immunoglobulin A
IgG	immunoglobulin G
IQR	interquartile range
J	joining
m.o.i.	multiplicity of infection
M	matrix
M2e	N-terminal extracellular domain of matrix 2
MAb	monoclonal antibody
mAU	milli-absorbance units
MDCK	Madin-Darby canine kidney
MEM	Eagle's minimum essential medium

m-IgA	monomeric immunoglobulin A
NA	neuraminidase
NI	neuraminidase inhibition
NP	nucleoprotein
OD	optical density
PBS	phosphate-buffered saline
PBST	phosphate-buffered saline containing 0.05% Tween 20
PCR	polymerase chain reaction
PFU	plaque forming unit
p-IgA	polymeric IgA
pIgR	polymeric immunoglobulin receptor
PR8	A/Puerto Rico/8/1934 (H1N1)
PVDF	polyvinylidene fluoride
RNA	ribonucleic acid
rpm	round per minute
RT	reverse transcription
SA1	A/shearwater/South Australia/1/1972 (H6N5)
SC	secretory component
SDS	sodium dodecyl sulfate
SPR	surface plasmon resonance
t/q-IgA	trimeric/tetrameric immunoglobulin A
TEM	transmission electron microscopy
TMB	3,3’,5,5’-tetramethylbenzidine
VH	variable gene segments for the heavy chain
VL	variable gene segments for the light chain

Notes

The contents of Chapter I have been published in Journal of Virology.

Okuya K, Yoshida R, Manzoor R, Saito S, Suzuki T, Sasaki M, Saito T, Kida Y, Mori-Kajihara A, Kondoh T, Sato M, Kajihara M, Miyamoto H, Ichii O, Higashi H, and Takada A. Potential role of nonneutralizing IgA antibodies in cross-protective immunity against influenza A viruses of multiple hemagglutinin subtypes. J Virol. 94, e00408-20, 2020.

The contents of Chapter II have been published in Viruses.

Okuya K, Eguchi N, Manzoor R, Yoshida R, Saito S, Suzuki T, Sasaki M, Saito T, Kida Y, Mori-Kajihara A, Miyamoto H, Ichii O, Kajihara M, Higashi H, and Takada A. Comparative analyses of the antiviral activities of IgG and IgA antibodies to influenza A virus M2 protein. Viruses 12, 780, 2020.

Preface

Influenza A viruses (IAVs) belonging to the family *Orthomyxoviridae* have eight-segmented, negative-sense, single-stranded RNA genomes. IAVs have two envelope glycoproteins, hemagglutinin (HA) and neuraminidase (NA), on the viral surface. IAV HA precursor HA0 is post-translationally cleaved into HA1 and HA2 subunits by host proteases (29, 63). HA1 mediates virus binding to sialic acids to initiate viral entry through endocytosis. The acidic pH in endosomes induces an irreversible conformational change in HA2 that mediates the fusion of the viral envelope and endosomal membranes (61). NA promotes the release of progeny virus particles from infected cells as well as the penetration through host mucus by desialylation of viral and cellular surface glycans (9, 54). NA also plays a role in the initial stage of virus infection by facilitating virus motility on the cell surface (51). HA and NA of IAVs are divided into 16 and 9 subtypes, respectively, based on their antigenicities (40). In addition, two novel influenza viruses were detected in bats captured in South and Central America and tentatively designated as new subtypes (H17N10 and H18N11) (72,80).

The matrix (M) gene of IAVs encodes two viral proteins, M1 and M2. The M1 protein is one of the most abundant structural components in IAV particles present on the inner leaflet of the viral envelope (3). The M2 protein is a tetrameric integral membrane protein having an N-terminal extracellular domain (M2e) of 24 amino acids, a transmembrane domain of 19 amino acids, and a cytoplasmic tail of 54 amino acids (20). The M2 protein possesses ion channel activity which is important for virus entry (13). Besides the ion channel activity, the M2 protein possesses membrane scission activity, which is necessary to pinch off newly produced virus particles during the budding process (56).

Immunoglobulin A (IgA) antibodies exist as monomeric and polymeric forms comprising two or more monomeric IgA (m-IgA) units covalently linked by a joining (J) chain (2, 26). Polymeric IgA (p-IgA) antibodies are intracellularly transferred to the apical membrane via transcytosis mediated by the polymeric immunoglobulin receptor (pIgR) expressed on the basolateral membrane, subsequently released from cells with the extracellular portion of pIgR, the so-called secretory component (SC), and function as secretory IgA on mucosal surfaces (50). Although several different forms of IgA molecules (i.e., monomeric, dimeric, trimeric, and tetrameric) are known, the majority of p-IgA molecules are dimeric (65). Secretory IgA antibodies contribute to mucosal immunity against IAVs by blocking the initial virus infection of epithelial cells in the respiratory tract (18, 43, 65) as well as inhibiting the viral egress from infected cells, most likely due to tethering of the progeny virus particles (42). Interestingly, it has been shown

that intranasal vaccination of mice with inactivated IAV particles provides cross-protective immunity against IAVs of multiple HA subtypes, whereas subcutaneous vaccination is only effective against the IAV homologous to the vaccine strain (66, 67). Since subcutaneous immunization predominantly induces a serum immunoglobulin G (IgG) response whereas intranasal immunization induces both IgG and IgA responses, p-IgA antibodies are suggested to play an important role in this heterosubtypic immunity (66, 67, 75). However, the mechanisms of heterosubtypic antiviral activity of IgA antibodies are not completely understood.

The purpose of this thesis is to reveal the mechanisms by which IgA antibodies contribute to the cross-protective immunity against multiple HA subtypes of IAVs. I particularly focused on nonneutralizing antibodies and compared antiviral activities between IgG and IgA antibodies. The present thesis consists of two chapters. In chapter I, it is shown that an HA-specific IgA antibody that has no neutralizing activity but exhibits broad binding capacity to multiple HA subtypes inhibits the release of IAV particles from the infected cells. In chapter II, it is demonstrated that an IgA antibody specific to the M2 protein, which is antigenically highly conserved irrespective of the HA subtype, reduced the amount of progeny viruses mostly likely due to inhibiting the budding or particle formation process of IAVs.

Chapter I:
Potential role of nonneutralizing IgA antibodies specific to hemagglutinin in cross-protective immunity against influenza A viruses

Introduction

The HA molecule is the major target of neutralizing antibodies, which predominantly bind to highly variable antigenic regions surrounding the receptor binding site of HA and inhibit viral entry into the cells (5, 52, 73). Since the antigenicity of HA is principally determined by the structure of the antigenic sites, the majority of neutralizing antibodies naturally produced upon infection and/or vaccination are HA subtype-specific and only a small population of neutralizing antibodies is known to recognize multiple HA subtypes (11, 14, 16, 53, 82). On the other hand, HA-specific neutralizing antibodies that do not inhibit receptor binding, as well as nonneutralizing antibodies, are also induced to other antigenic regions (e.g., stem regions) conserved among multiple HA subtypes (14, 16, 41, 59).

IAV HA-specific IgA antibodies are thought to contribute to cross-protective immunity against multiple IAV subtypes. However, the mechanisms by which IgA exerts such versatile antiviral activity are not fully understood. In this chapter, I focused on HA-specific but broadly cross-reactive nonneutralizing p-IgA antibodies since such antibodies are known to be generally present in immunized mice (41), whereas HA-specific cross-reactive antibodies with "classical" neutralizing capacity (i.e. inhibition of viral entry into cells) are limitedly induced. Recombinant IgG, m-IgA, and p-IgA antibodies were generated based on the sequence of a mouse anti-HA monoclonal antibody (MAb) 5A5 that had no neutralizing activity but showed a broad binding capacity to multiple HA subtypes. Antiviral activities other than neutralization among the three forms of antibodies were compared using IAVs of various HA subtypes *in vitro*.

Materials and Methods

Cells and viruses

Madin-Darby canine kidney (MDCK) cells were maintained in Eagle's minimum essential medium (MEM; Sigma-Aldrich, St. Louis, MO, USA) supplemented with 10% bovine serum (Gibco, Waltham, MA, USA), 100 U/ml penicillin, and 0.1 mg/ml streptomycin (Gibco, Waltham, MA, USA). Human embryonic kidney (HEK) 293T cells were grown in Dulbecco's modified Eagle's medium (DMEM) (Sigma-Aldrich, St. Louis, MO, USA) supplemented with 10% fetal bovine serum (FBS) (Sigma-Aldrich, St. Louis, MO, USA), 100 U/ml penicillin, and 0.1 mg/ml streptomycin (Gibco, Waltham, MA, USA). After IAVs inoculation, MDCK cells were cultured in MEM containing 0.3% bovine serum albumin (0.3% BSA/MEM) with 5 μg/ml trypsin (Gibco, Waltham, MA, USA). Expi 293F cells were maintained in Expi293 Expression Medium (Thermo Fisher Scientific, Waltham, MA, USA) as described in the manufacturer's instructions. MDCK and HEK 293T cells were maintained at 37ºC in 5% CO_2. Expi 293F cells were maintained at 37ºC in 8% CO_2 while being shaken with a 125 round per minute (rpm) orbital shaker. A/Puerto Rico/8/1934 (H1N1) (PR8) and A/Adachi/2/1957 (H2N2) (Ad2) were propagated in MDCK cells. A/Hong Kong/483/1997 (H5N1) (HK483), A/shearwater/South Australia/1/1972 (H6N5) (SA1), A/duck/England/1/1956 (H11N6) (Eng1), and A/duck/Alberta/60/1976 (H12N5) (Alb60) were propagated in embryonated chicken eggs. All viruses were stored at −80°C until use. Infectious titers were determined by a plaque-forming assay with MDCK cells. The use of infectious materials was approved by the Committee for Safety Management of Pathogens, Research Center for Zoonosis Control (CZC), Hokkaido University (HU) (10[07]).

Production of mouse MAb 5A5

Six-week-old female BALB/c mice were subcutaneously immunized twice at 2-week intervals with 100 μg of formalin (0.2%)-inactivated purified Eng1 together with complete Freund's adjuvant (Difco Laboratories, Detroit, MI, USA). Three weeks after the second immunization, the mice were intraperitoneally boosted with inactivated virus alone. Three days later, spleen cells from the mice and mouse myeloma P3U1 cells were fused and maintained according to a standard procedure (27). Hybridomas were screened for secretion of influenza virus-specific MAb by enzyme-linked immunosorbent assay (ELISA), and then HA-specific MAbs were identified by Western blotting and immunostaining of HEK 293T cells transfected with plasmids expressing Eng1 HA. MAbs reactive to Eng1 were further screened for their cross-reactivity to other HA subtypes by ELISA, and I obtained cross-reactive MAb 5A5 (IgG1). The hybridoma

producing MAb 5A5 (IgG1) was cloned three times by limiting dilution of the cells. Animal studies were carried out in strict accordance with the Guidelines for Proper Conduct of Animal Experiments of the Science Council of Japan. The protocol was approved (08-0235) by the Hokkaido University Animal Care and Use Committee.

5'-rapid amplification of cDNA ends (5'-RACE)-PCR and sequence

Total RNA was extracted from the hybridoma producing mouse MAb 5A5 using an RNeasy kit (Qiagen, Hilden, Germany) and reverse transcribed with a SMARTer RACE 5'/3' kit (Clontech, Shiga, Japan) using 5' RACE CDS primer A (Clontech, Shiga, Japan). Subsequently, the variable gene segments for the heavy chain (VH) and light chain (VL) were amplified by PCR with the primer sets specific to VH and VL, respectively, using SeqAmp DNA polymerase according to the manufacturer's instructions (Takara, Shiga, Japan). The PCR products for the VH and VL genes were cloned into a vector, pCR-Blunt II-TOPO (Invitrogen, Carlsbad, CA, USA), and subjected to nucleotide sequencing. The nucleotide sequences were determined by using a BigDye Terminator sequencing kit, version 3.1 (Applied Biosystems, Foster City, CA, USA) and Applied Biosystems 3130xl Genetic Analyzer (Applied Biosystems, Foster City, CA, USA). The primer sequences are available upon request.

Expression and purification of MAbs

VH and VL genes of MAbs 5A5 and B12 were amplified with restriction enzyme cutting sites and ligated into α1H, γ1HC, and κLC vectors (58, 71) by using ligation mix (Takara, Shiga, Japan) as described in the manufacturer's instructions. To express a human-mouse chimeric IgG antibody, Expi 293F cells were cotransfected with γ1HC- and κLC-expressing plasmids using an Expifectamine 293 Transfection kit (Gibco, Waltham, MA, USA). To express human-mouse chimeric IgA antibodies, Expi 293F cells were cotransfected with α1H-, κLC-, J chain-, and SC-expressing plasmids (58). After culture for 5 days, supernatants were collected and subjected to purification of the antibodies. IgG and IgA antibodies were purified from Expi 293F cell supernatants by using UNOsphere SUPrA (BioRad, Hercules, CA, USA) and CaptureSelect IgA (Invitrogen, Carlsbad, CA, USA), respectively. Each antibody was concentrated using Amicon Ultra 30K (Merck Millipore, Darmstadt, Germany). For IgG antibodies, elution buffer was replaced with phosphate-buffered saline (PBS) during the concentration process. Concentrated IgA antibodies were further subjected to gel filtration chromatography (GFC) using a Superose 6 10/300 GL column (GE Healthcare, Little Chalfont, UK) with an AKTA avant 25 chromatography system (GE Healthcare, Little

Chalfont, UK). Fractionated samples were analyzed by blue native polyacrylamide gel electrophoresis (BN-PAGE) using NativePAGE 4–16% Bis-Tris Protein Gels (Invitrogen, Carlsbad, CA, USA). NativeMark (Invitrogen, Carlsbad, CA, USA) was used as a molecular weight standard. Considering the results of BN-PAGE, fractions were separated into two subsets: m-IgA and p-IgA antibodies. Fractions for each IgA antibody subset were pooled and concentrated using Amicon Ultra 30K (Merck Millipore, Darmstadt, Germany). All antibodies were stored at −80°C until use. The use of recombinant antibodies was approved by Hokkaido University Safety Committee for Genetic Recombination Experiments (21[4]).

Expression of recombinant HA

Recombinant HAs for ELISA antigens were prepared as previously reported (41). Briefly, HEK 293T cells transfected with the protein expression vector pCAGGS (48) encoding recombinant HAs using TransIT-LT1 (Mirus, Madison, WI, USA) were subjected to membrane protein extraction using a eukaryotic membrane protein extraction reagent kit (Thermo Fisher Scientific, Waltham, MA, USA). HA protein antigens of the following IAVs were prepared: A/swine/Hokkaido/2/1981 (H1N1), PR8, A/Kadoma/4/2006 (H1N1), A/Narita/1/2009 (H1N1), Ad2, A/Aichi/2/1968 (H3N2), A/duck/Hokkaido/5/1977 (H3N2), A/duck/Czechoslovakia/1956 (H4N6), HK483, A/duck/Hong Kong/820/1980 (H5N3), SA1, A/duck/Hokkaido/301/1978 (H7N2), A/seal/Massachusetts/1/1980 (H7N7), A/turkey/Ontario/6118/1968 (H8N4), A/Hong Kong/1073/1999 (H9N2), A/chicken/Germany/N/1949 (H10N7), Eng1, Alb60, A/gull/Maryland/704/1977 (H13N6), A/mallard/Astrakhan/263/1982 (H14N5), A/duck/Australia/341/1983 (H15N8), A/black-headed gull/Sweden/5/1999 (H16N3), and A/little yellow-shouldered bat/Guatemala/060/2010 (H17N10). To generate chimeric HAs (cHAs; cHA H1/17 and cHA H17/1) between PR8 and A/little yellow-shouldered bat/Guatemala/060/2010 (H17N10), cDNAs corresponding to the HA globular head and the other regions were amplified and cloned into the pCAGGS vector (48) using an In-Fusion HD Cloning Kit (Clontech, Shiga, Japan). The extracted membrane proteins were appropriately diluted with PBS to give the highest optical density (OD) values at 450 nm for hyperimmune chicken antisera (repository of Division of Global Epidemiology, CZC, HU) (41) specific to the respective HA subtypes and used as antigens for ELISA. The use of recombinant antibodies was approved by Hokkaido University Safety Committee for Genetic Recombination Experiments (21[4]).

ELISA

ELISA plates (Nunc Maxisorp, Invitrogen, Carlsbad, CA, USA) were coated with the prepared HA antigens and blocked with PBS containing 3% skim milk (Becton Dickinson, Franklin Lakes, NJ, USA). MAb 5A5 diluted in 1% skim milk in PBS containing 0.05% Tween 20 (PBST) were plated in triplicate, and bound antibodies were detected using horseradish peroxidase (HRP)-conjugated goat anti-human IgG (H+L) (109-001-003, Jackson Immuno Research, West Grove, PA, USA) or HRP-conjugated goat anti-human IgA (H+L) (ab97215, Abcam, Cambridge, UK). The reaction was visualized by adding 3,3',5,5'-tetramethylbenzidine (TMB; Sigma-Aldrich, St. Louis, MO, USA) and absorbance at 450 nm was measured.

Surface plasmon resonance (SPR) assay

SPR assay was performed by using Biacore 3000 (GE Healthcare, Little Chalfont, UK) as described in a previous study (58). Briefly, recombinant trimeric PR8 HA with a C-terminal His-tag was immobilized on the surface of Sensor Chip NTA (GE Healthcare, Little Chalfont, UK) by using the NTA reagent kit (GE Healthcare, Little Chalfont, UK). After trimeric HA immobilization (10 μg/ml), the molecular interaction of HA with MAb 5A5 IgG, m-IgA, or p-IgA (50 μg/ml) was analyzed.

Neutralization assay

IAVs (50–100 plaque forming units [PFU]) were incubated with serial dilutions of antibodies (0.01–100 μg/ml) prior to inoculation into MDCK cells. The following antibodies were selected from the repository of Division of Global Epidemiology, CZC, HU, and used as positive control neutralizing antibodies: anti-H1 MAb APH 269-5, anti-H2 MAb S139/1 (42, 82), anti-H5 MAb 36-1, anti-H6 MAb 85-2-2, anti-H11 MAb 9F5-2-4, and anti-H12 MAb 15-3-1. After incubation with the viruses, the cells were washed with PBS twice and overlaid with 0.3% BSA/MEM containing 1.2% Avicel RC 591 (FMC BioPolymer, Philadelphia, PA, USA) (36), a processed mixture of microcrystalline cellulose and sodium carboxymethyl cellulose, and 5 μg/ml trypsin. After 20-hour incubation, the cells were fixed with methanol and blocked with PBS containing 1% BSA. Plaques were stained with a mouse anti-HA MAb, HRP-conjugated goat anti-mouse IgG (H+L) (115-035-062, Jackson Immuno Research, West Grove, PA, USA), and a 3,3'-diaminobenzidine substrate (Wako, Osaka, Japan).

Sample collection of cell lysates and supernatants of infected cells

MDCK cells seeded on 12-well plates (Corning, Corning, NY, USA) were incubated with IAVs at a multiplicity of infection (m.o.i.) of 2.0 for an hour for adsorption,

and then washed with PBS three times. Subsequently, the infected cells were incubated with culture media containing 10 μg/ml of IgG and IgA forms of MAb 5A5 or the control antibody (MAb B12). Eight hours later, the supernatant was centrifuged (15,000 × g, 4°C, 10 min) and collected to new tubes. Laemmli sample buffer (BioRad, Hercules, CA, USA) containing 2-mercaptoethanol was added to the cells and collected into tubes.

Western blotting

Cells and supernatants that were mixed with Laemmli sample buffer (BioRad, Hercules, CA, USA) containing 2-mercaptoethanol were incubated at 95°C for 10 and 5 minutes, respectively. After sodium dodecyl sulfate (SDS)-PAGE using 12% SDS, separated proteins were transferred onto polyvinylidene fluoride (PVDF) membranes (Merck Millipore, Darmstadt, Germany). The PVDF membranes were blocked with PBS containing 3% skim milk (Becton Dickinson, Franklin Lakes, NJ, USA) and washed with PBST. Each membrane was incubated with a mouse anti-M1 MAb (APH 6-23-1-6) (44) and a mouse anti-beta actin antibody (ab6276, Abcam, Cambridge, UK) as primary antibodies and HRP-conjugated goat anti-mouse IgG (H+L) (115-035-062, Jackson Immuno Research, West Grove, PA, USA) as a secondary antibody. Antibodies were diluted with PBST containing 1.5% skim milk. After washing with PBST, the bound antibodies were visualized with Immobilon Western (Merck Millipore, Darmstadt, Germany). The amount of the viral M1 protein was semi-quantified from the intensity of the stained band using an Amersham Imager 600 (GE Healthcare, Little Chalfont, UK).

Real-time reverse transcription (RT) -PCR

Viral RNA was extracted from the cell supernatant using a QIAmp Viral RNA Mini Kit (Qiagen, Hilden, Germany) and subjected to real-time RT-PCR-based IAV gene detection using a One step SYBR prime script RT-PCR kit II (Takara, Shiga, Japan). Primer sets specific for conserved regions of IAV nucleoprotein (NP) genes (NP 972F [CAAGAGTCAGCTGGTGTGGA] and NP 1160R [GCCCAGTACCTGCTTCTCAG]) were used. Quantitation of the NP gene was performed using a standard curve generated by threshold cycle values obtained from 10-fold serial dilutions (covering 10^2 to 10^6 copies) of the PR8 NP gene inserted into the pHH21 vector (47). All samples were tested in triplicate. Average copy numbers of the viral genome in the supernatant of IAV-infected cells incubated without any MAb was set to 100%. Real-time RT-PCR conditions are available upon request.

Transmission electron microscopy (TEM)

TEM was performed as described previously (42, 49). Briefly, MDCK cells infected with IAVs at m.o.i. 1.0–2.0 were cultured with or without MAb 5A5 IgG, m-IgA, or p-IgA (10 μg/ml) for eight hours and fixed with 2.5% glutaraldehyde in 0.1 M cacodylate buffer (pH 7.4). The fixed cells were postfixed with 2% osmium tetroxide, dehydrated with series of ethanol gradients followed by propylene oxide, embedded in Epon 812 Resin mixture (TAAB Laboratories Equipment Ltd., Berks, UK), and polymerized. Ultrathin sections (50 nm) were stained with uranyl acetate and lead citrate and examined with a JEM-1210 (JEOL, Tokyo, Japan) electron microscope at 80 kV.

NA inhibition (NI) assay

NI assays based on the enzyme-linked lectin assay (ELLA) method were performed as described previously (4, 33, 79). Briefly, ELISA plates (Nunc Maxisorp, Invitrogen, Carlsbad, CA, USA) were coated with 100 μl of fetuin (Wako, Osaka, Japan) at a concentration of 500 μg/ml and blocked with PBS containing 5% BSA. MAbs 5A5 IgG and IgA were two-fold serially diluted from 200 μg/ml in PBS and reacted with the viruses diluted to 2 × 50% effective concentration (based on NA assay) in PBS containing 1% BSA. Chicken hyperimmune antisera against A/duck/Hokkaido/Vac-1/04 (H5N1), A/Singapore/1/1957 (H2N2), A/mallard/Astrakhan/263/1982 (H14N5), and Eng1 (H11N6) was used as positive control antibodies. Antibody-virus mixture was transferred to fetuin-coated plates. A secondary solution of peanut agglutinin conjugated with peroxidase (Sigma-Aldrich, St. Louis, MO, USA) was added at a concentration of 1 μg/ml in PBS. The reaction was visualized by adding the TMB (Sigma-Aldrich, St. Louis, MO, USA) solution and absorbance at 450 nm was measured.

Plaque size reduction assay

Confluent monolayers of MDCK cells on 12-well plates (Corning, Corning, NY, USA) were infected with the viruses to give 50–100 PFU and overlaid with 0.3% BSA/MEM containing 5 μg/ml trypsin, 10 μg/ml of IgG and IgA forms of MAb 5A5 and the control antibody (MAb B12), and 0.8% agarose S (Wako, Osaka, Japan). After incubation with or without MAbs for two days at 35°C, plaques were visualized by immunostaining using the same methods as described for the neutralizing assay above. Plaque images on the wells were scanned and sizes of at least 30–50 plaques were measured using ImageJ analysis software.

Statistical analyses

Data (band intensity, RNA copy number, and plaque size) were analyzed using GraphPad Prism version 8 for Windows (GraphPad Software, San Diego, CA, USA). One-way analysis of variance (ANOVA) followed by Tukey's multiple comparison test was used to analyze each data set as indicated in the figure legends. The following statistical values and symbols are used throughout the manuscript; *$p < 0.05$, **$p < 0.01$, ***$p < 0.001$; ****$p < 0.0001$.

Results

Production of monoclonal IgG and IgA antibodies

Mouse MAb 5A5, which is highly cross-reactive to multiple HA subtypes but has no neutralizing activity, was selected from the repository of Division of Global Epidemiology, CZC, HU. To compare the antiviral activities of IgG and IgA forms of this antibody, mouse-human chimeric IgG and IgA antibodies were generated based on the sequence of the mouse MAb 5A5 variable region. Briefly, the genes encoding variable regions of this antibody were cloned into heavy and light chain expression plasmids and the constructed plasmids were subsequently transfected into Expi 293F cells. Note that SC and J chain expression plasmids were co-transfected to generate p-IgA antibodies. Recombinant IgG and IgA antibodies were purified from the supernatant by affinity chromatography. Then GFC enabled us to separate different forms of IgA antibodies based on their molecular weights (Fig. 1A). Fractions 1–9 and 12–14 were pooled for MAb 5A5 p-IgA and m-IgA, respectively. Negative control IgG and IgA antibodies were produced in the same manner based on the sequence of MAb B12, which was obtained from a healthy adult volunteer (58) (Fig. 1B). Fractions 1–8 and 10–14 were pooled for MAb B12 p-IgA and m-IgA, respectively (Fig. 1B). The purified MAbs were validated for their purity and molecular weight (Fig. 1C and D) and used for further analyses.

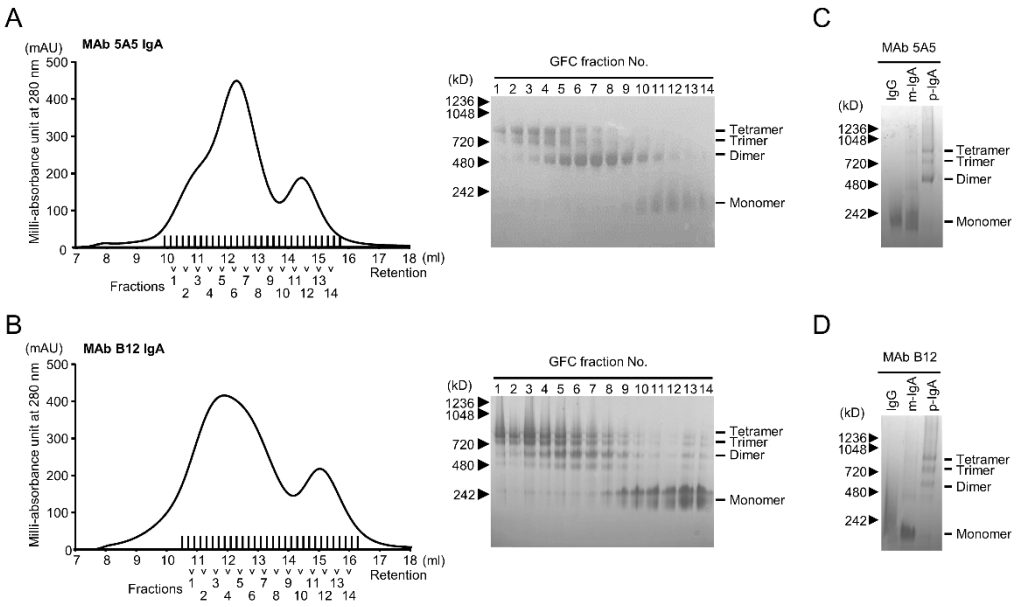

Figure 1 Purification of chimeric MAb 5A5 IgG and IgA

Recombinant IgG and IgA antibodies were purified from the supernatant by affinity chromatography. MAb 5A5 (A) and B12 (B) IgA antibodies were further fractionated by GFC with a Superose 6 10/300 GL column. A chromatogram demonstrating absorbance at 280 nm (shown in milli-absorbance unit) revealed two major peaks. Fractions covering the two peaks were subjected to BN-PAGE. Equal amounts (5 μg) of purified IgG, m-IgA, and p-IgA from MAb 5A5 (C) and B12 (D) were used for BN-PAGE.

Broad cross-binding capacity of MAb 5A5 IgG and IgA to multiple HA subtypes

The binding capacities and specificities of recombinant MAb 5A5 IgG and IgA were investigated by ELISA methods using HA antigens of H1–H17 subtypes (Fig. 2A). MAb 5A5 IgG, m-IgA, and p-IgA showed similar binding patterns to HA subtypes (H1, H2, H4, H5, H6, H7, H8, H9, H10, H11, H12, H14, and H15), confirming that these recombinant IgG and IgA MAbs shared the antigen-binding site and recognized the same epitope. MAb 5A5 did not show reactivity to H3, H13, H16, H17, and B/Lee strains. To obtain information on the epitope of MAb 5A5, two cHAs between PR8 and A/little yellow-shouldered bat/Guatemala/060/2010 (H17N10) as representative MAb 5A5 reactive and nonreactive virus strains, respectively, were generated (Fig. 2A): cH1/17 comprised of a part of the HA1 region (amino acid positions 52–277), the so-called the globular head region which contains the sialic acid receptor binding site (19, 62), from PR8 and the other region, a portion of HA1 regions and HA2 which drives membrane fusion, from the H17N10 virus, and vice versa (Fig. 2B). MAb 5A5 IgG, m-IgA, and p-IgA were found to recognize the globular head region of H1 HA in ELISA (Fig. 2C). Based on the reactivities of the antibodies, three IAV strains each were selected as representative human and avian isolates for further analyses: PR8, Ad2, and HK483 (human), SA1, Eng1, and Alb60 (avian), respectively.

Then, the binding activity among MAb 5A5 IgG, m-IgA, and p-IgA against HAs derived from the selected 6 IAV strains was compared. Although MAb 5A5 IgG showed slightly lower reactivity to PR8 HA than m-IgA and p-IgA, there was no remarkable difference in the binding capacity to other HAs in ELISA (Fig. 3A). To quantify avidity of each MAb to PR8 HA, the binding dynamics of MAb 5A5 IgG, m-IgA, and p-IgA was investigated by SPR analysis. It was revealed that MAb 5A5 p-IgA showed only a slightly lower dissociation rate than IgG and m-IgA (Fig. 3B). These results indicated that the isotype difference between IgG1 and IgA1 backbones gave only limited effects on the binding activity of MAb 5A5 while polymerization might slightly enhance the avidity of MAb 5A5.

It was confirmed that MAb 5A5 IgG, m-IgA, and p-IgA did not show neutralizing activity against any of the six IAVs tested (Fig. 4). Since nonneutralizing antibodies may have the potential to interfere with the virus budding/release process (40, 58), inhibitory effects of these MAbs on virus release from MDCK cells infected with IAVs were investigated (Fig. 5). Significantly lower amounts of the M1 protein in the supernatants of PR8-, HK483-, SA1-, and Eng1-infected cells incubated with MAb 5A5 m-IgA and p-IgA than in those of MAb-untreated cells were detected, and p-IgA decreased the M1 amount more significantly than IgG or m-IgA (Fig. 5A). MAb 5A5 IgG

showed inhibitory effects only against HK483 and Eng1. MAb B12 IgG, m-IgA, and p-IgA showed no remarkable inhibitory effects. There was no significant difference in the intracellular expression levels of the M1 protein of these six IAV strains among the antibody treatments, indicating that viral protein synthesis was not affected by the treatment with MAb 5A5 or the negative control antibody MAb B12 (Fig. 5B).

To further analyze the amounts of virus particles released into cell culture supernatants, viral RNAs (NP gene) were quantified by real-time RT-PCR assays. It was confirmed that the RNA copy numbers of the NP gene of PR8, HK483, SA1, Eng1, and Alb60 were significantly lower in the supernatants of the cells incubated with MAb 5A5 p-IgA than in those of the cells incubated with IgG or m-IgA (Fig. 6). Taken together, these results indicated that MAb 5A5 p-IgA had greater potential than IgG and m-IgA to reduce the number of IAV particles released from infected cells.

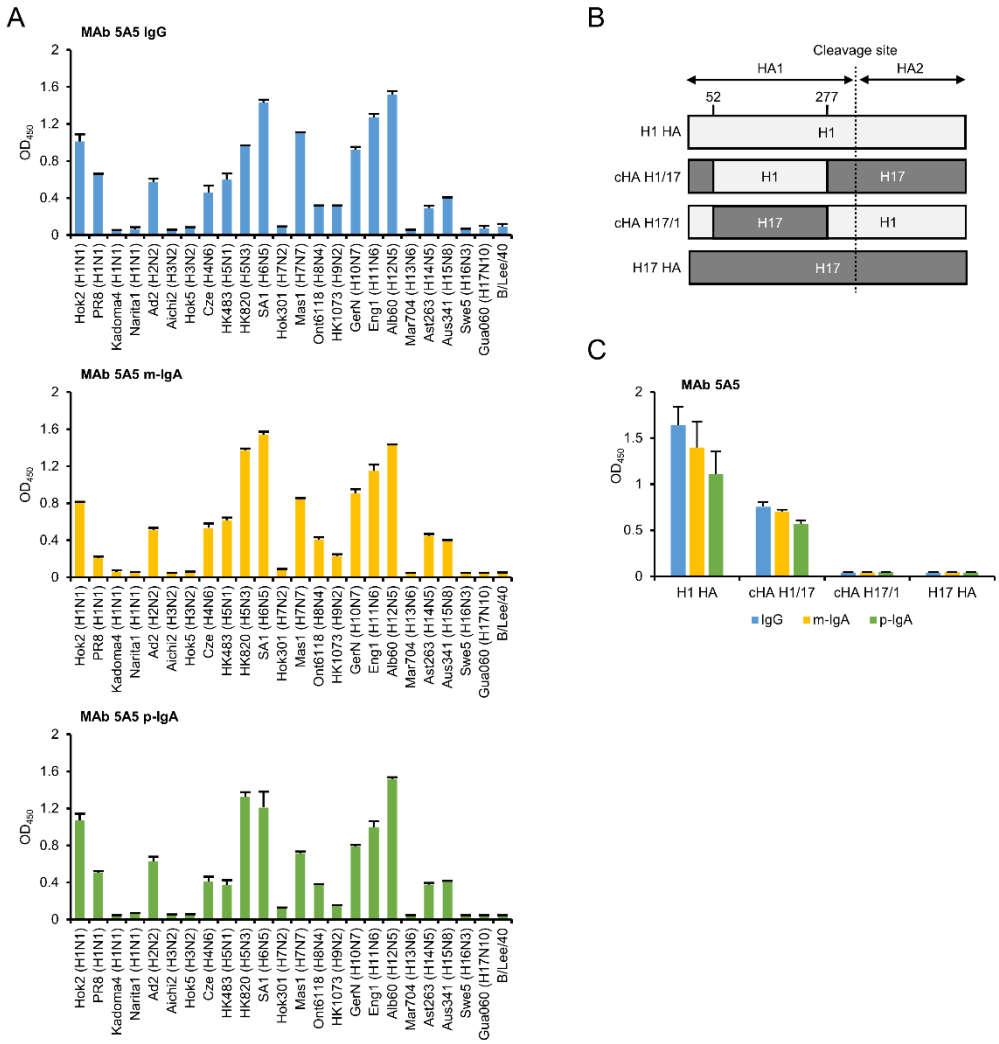

Figure 2 Reactivities of MAb 5A5 IgG, m-IgA, and p-IgA to HA antigens from various subtypes

Reactivities of MAb 5A5 IgG, m-IgA, and p-IgA to recombinant HAs were measured in ELISA (A). MAb 5A5 was diluted at 0.1 μg/ml before use. HAs of the following IAV strains were used: A/swine/Hokkaido/2/1981 (H1N1), A/Puerto Rico/8/1934 (H1N1), A/Kadoma/4/2006 (H1N1), A/Narita/1/2009 (H1N1), A/Adachi/2/1957 (H2N2), A/Aichi/2/1968 (H3N2), A/duck/Hokkaido/5/1977 (H3N2), A/duck/Czechoslovakia/1956 (H4N6), A/Hong Kong/483/1997 (H5N1), A/duck/Hong Kong/820/1980 (H5N3), A/shearwater/South Australia/1/1972 (H6N5), A/duck/Hokkaido/301/1978 (H7N2), A/seal/Massachusetts/1/1980 (H7N7), A/turkey/Ontario/6118/1968 (H8N4), A/Hong Kong/1073/1999 (H9N2), A/chicken/Germany/N/1949 (H10N7), A/duck/England/1/1956 (H11N6), A/duck/Alberta/60/1976 (H12N5), A/gull/Maryland/704/1977 (H13N6), A/mallard/Astrakhan/263/1982 (H14N5), A/duck/Australia/341/1983 (H15N8), A/black-

headed gull/Sweden/5/1999 (H16N3), and A/little yellow-shouldered bat/Guatemala/060/2010 (H17N10). An influenza B virus strain, B/Lee/1940, was used as a negative control. H1, H17, and cHAs were constructed as described in Materials and Methods (B). H1 and H17 HAs were derived from A/Puerto Rico/8/1934 (H1N1) and A/little yellow-shouldered bat/Guatemala/060/2010 (H17N10), respectively. Numbers indicate positions of amino acids in H3 numbering. Reactivities of MAb 5A5 IgG, m-IgA, and p-IgA to the cHAs were measured in ELISA (C). Columns and error bars indicate the means and standard deviations of triplicate wells, respectively.

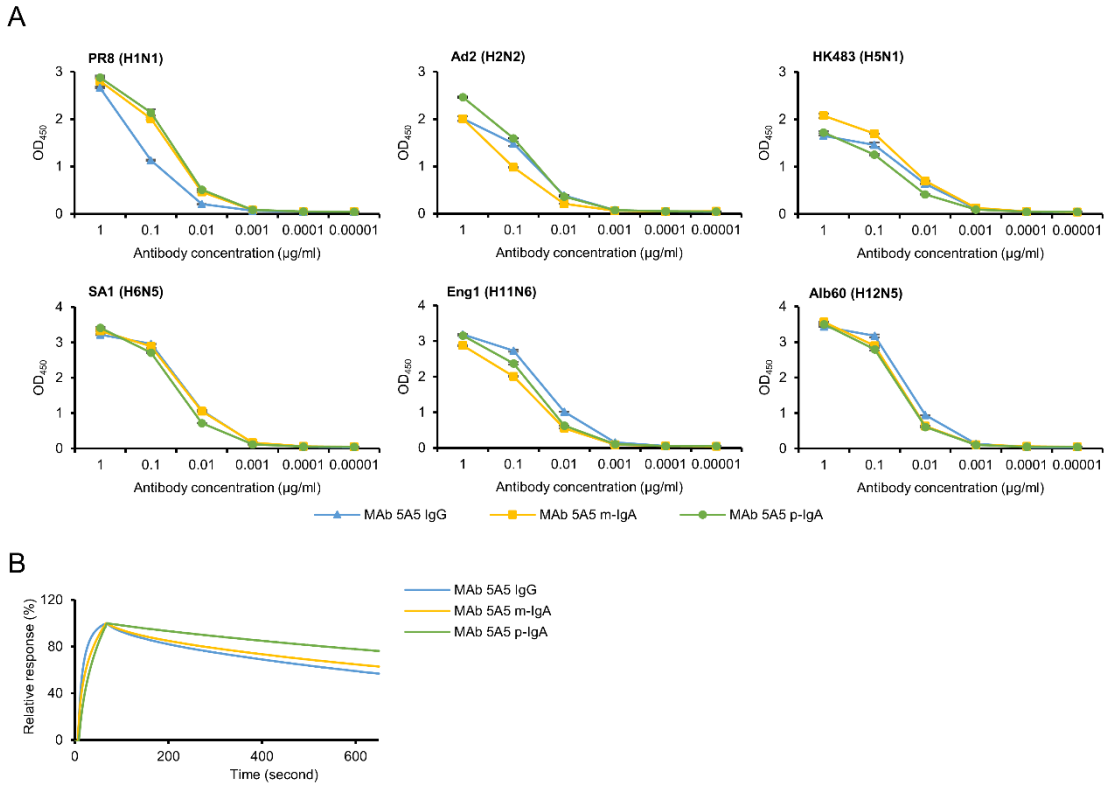

Figure 3 Comparison of avidity to HA antigens among MAb 5A5 antibodies

Reactivities of IgG, m-IgA, and p-IgA (0.00001–1 μg/ml) to recombinant HAs of PR8, Ad2, HK483, SA1, Eng1, and Alb60 were measured in ELISA (A). Binding dynamics of MAb 5A5 IgG, m-IgA, and p-IgA against the recombinant trimeric PR8 HA (B). Sensorgrams were adjusted (x=0, y=0: baseline, y=100: binding) to allow comparisons between different antibody forms in terms of the dissociation rate.

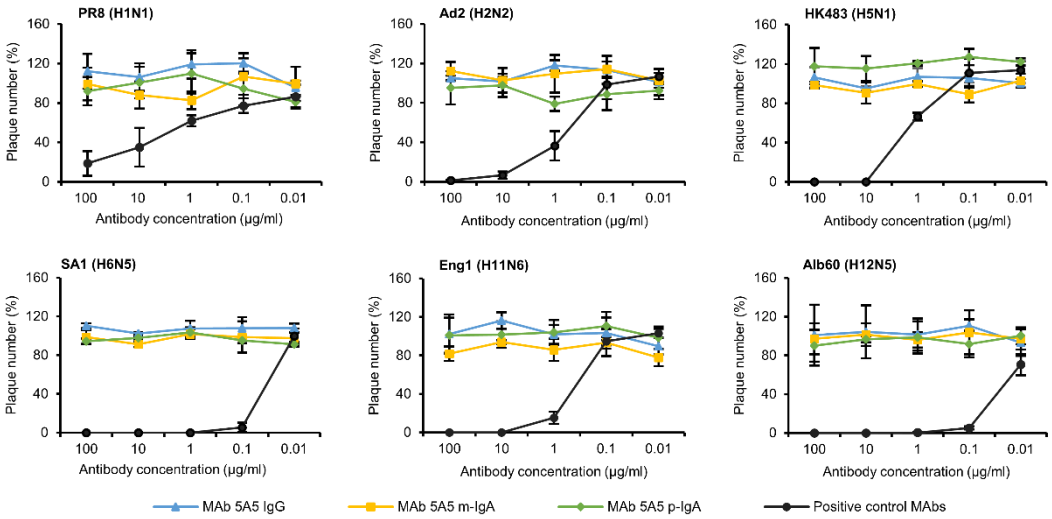

Figure 4 Neutralization tests of MAb 5A5 antibodies

Serial dilutions of MAb 5A5 IgG, m-IgA, p-IgA, and positive control neutralizing MAbs (0.01–100 μg/ml) were mixed with the respective IAV strains, followed by plaque assays as described in Materials and Methods. Means and standard deviations of plaque numbers were calculated from three individual experiments. Relative plaque numbers to each control sample (i.e. cells incubated without MAbs) are shown.

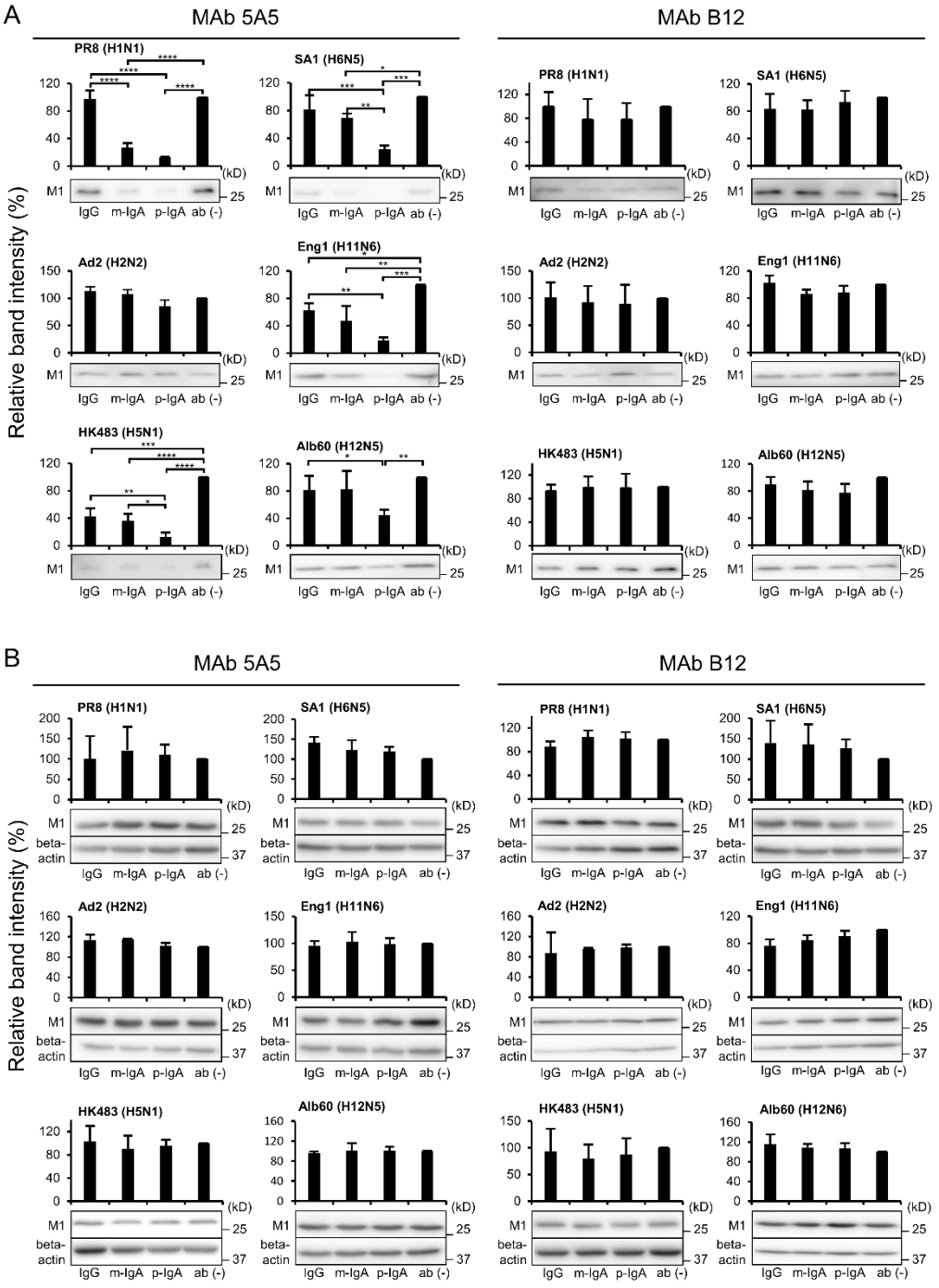

Figure 5 Detection of the viral protein in supernatants and lysates of IAV-infected cells

MDCK cells were infected with IAVs at an m.o.i. 2.0 and incubated with or without 5A5 and B12 MAbs (10 μg/ml). The M1 protein in supernatants (A) and cell lysates (B) was detected in Western blotting and beta-actin was also stained for cell lysate samples. Relative band intensities to each control sample (i.e., cells incubated without MAbs) are

shown. Each experiment was performed three times and averages and standard deviations are shown. Asterisks indicate significant differences (*$p < 0.05$, **$p < 0.01$, ***$p < 0.001$, ****$p < 0.0001$) found using one-way ANOVA followed by Tukey's multiple comparison tests.

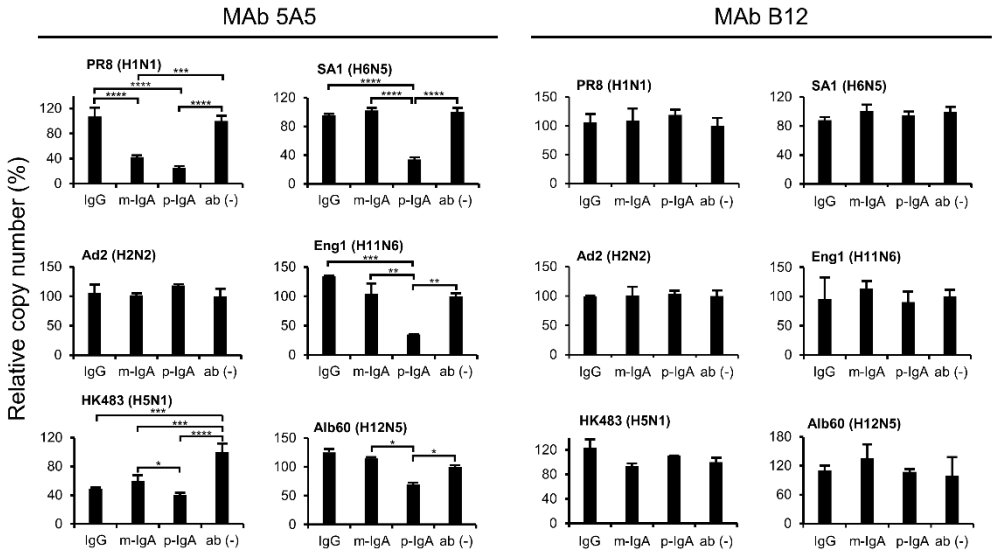

Figure 6 Detection of the viral RNA genome in supernatants of IAV-infected cells

MDCK cells were infected with IAVs at an m.o.i. 2.0 and incubated with or without 5A5 or B12 MAbs (10 μg/ml). The viral RNA genome was detected by real-time RT-PCR. Average copy numbers of the viral genome in the supernatant of IAV-infected cells incubated without any MAb was set to 100%. Each experiment was performed three times and averages and standard deviations are shown. Asterisks indicate significant differences (*$p < 0.05$, **$p < 0.01$, ***$p < 0.001$, ****$p < 0.0001$) determined using one-way ANOVA followed by Tukey's multiple comparison tests.

Accumulation of virus particles on IAV-infected cells incubated in the presence of MAb 5A5 IgA

To investigate the mechanism of the antiviral activities of the antibodies, IAV-infected MDCK cells incubated with MAb 5A5 IgG, m-IgA, and p-IgA were observed by TEM. Unusual aggregation and accumulation of virus particles were found on the virus-infected cells cultured in the presence of MAb 5A5 m-IgA and p-IgA, and this phenomenon was particularly prominent in the p-IgA-treated cells (Fig. 7). In contrast, lower numbers of virus particles in less proximity were found on the infected cells incubated with MAb 5A5 IgG and MAb-untreated cells, suggesting that efficient virus release from infected cells occurred. These data indicated that MAb 5A5 m-IgA and p-IgA deposited newly produced virus particles on the cell surface more efficiently than IgG, resulting in reduced virus release from infected cells. Since anti-HA antibodies that sterically hinder NA access to sialic acids were shown to possess NI activity (7), NI activity of MAb 5A5 IgA was investigated by ELLA (79). I confirmed that both m-IgA and p-IgA showed only minimum NI activities against the viruses even at the highest concentration (100 μg/ml) (Fig. 8). These results indicated that reduced virus release which was most likely caused by aggregation and accumulation of virus particles on the infected cells was not due to NI activity of MAb 5A5 IgA.

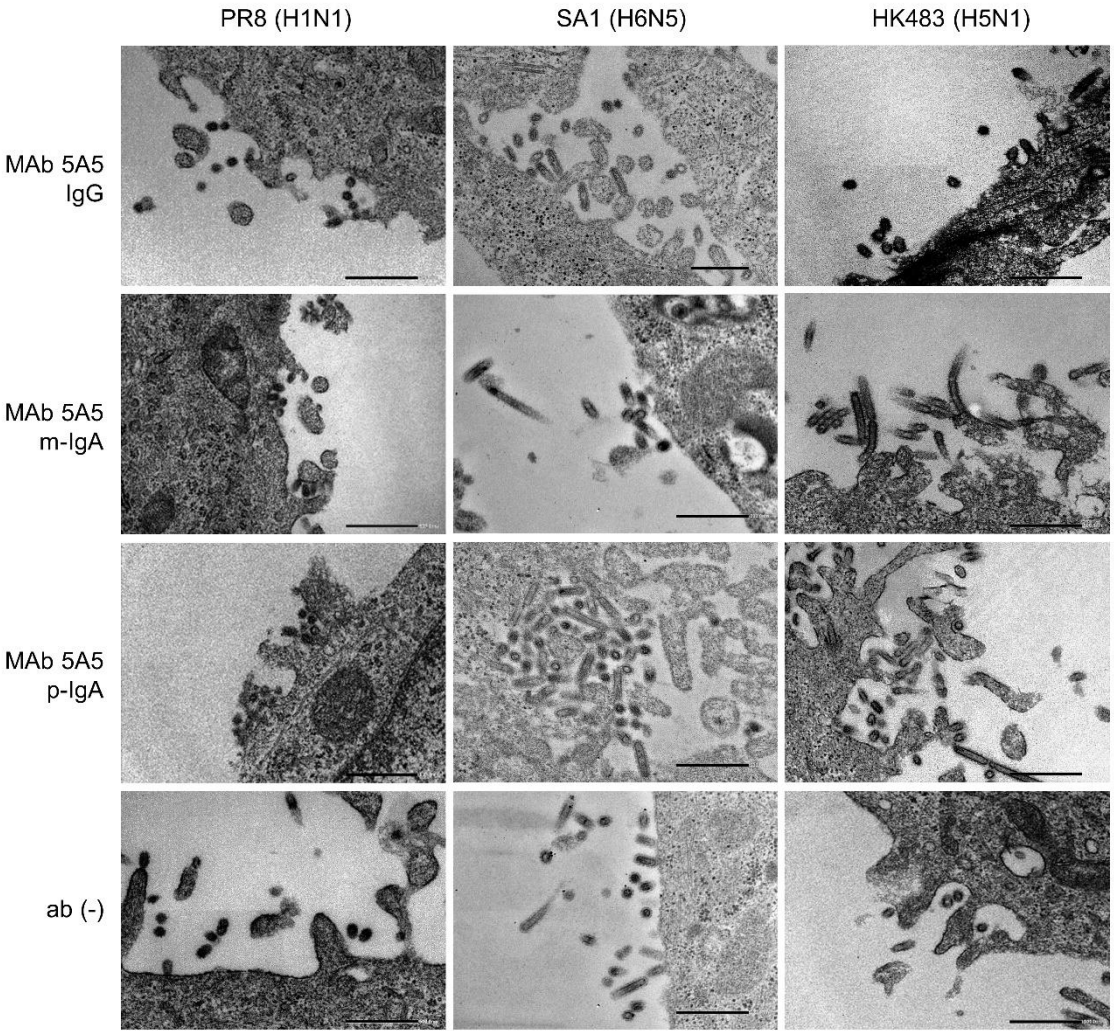

Figure 7 Electron microscopy of virus particles on IAV-infected cells

MDCK cells were infected with IAVs at an m.o.i. 2.0 and incubated for eight hours with or without MAb 5A5 IgG, m-IgA, or p-IgA. Randomly selected fields (10–20) were observed and representative images are shown. Scale bars represent 500 nm.

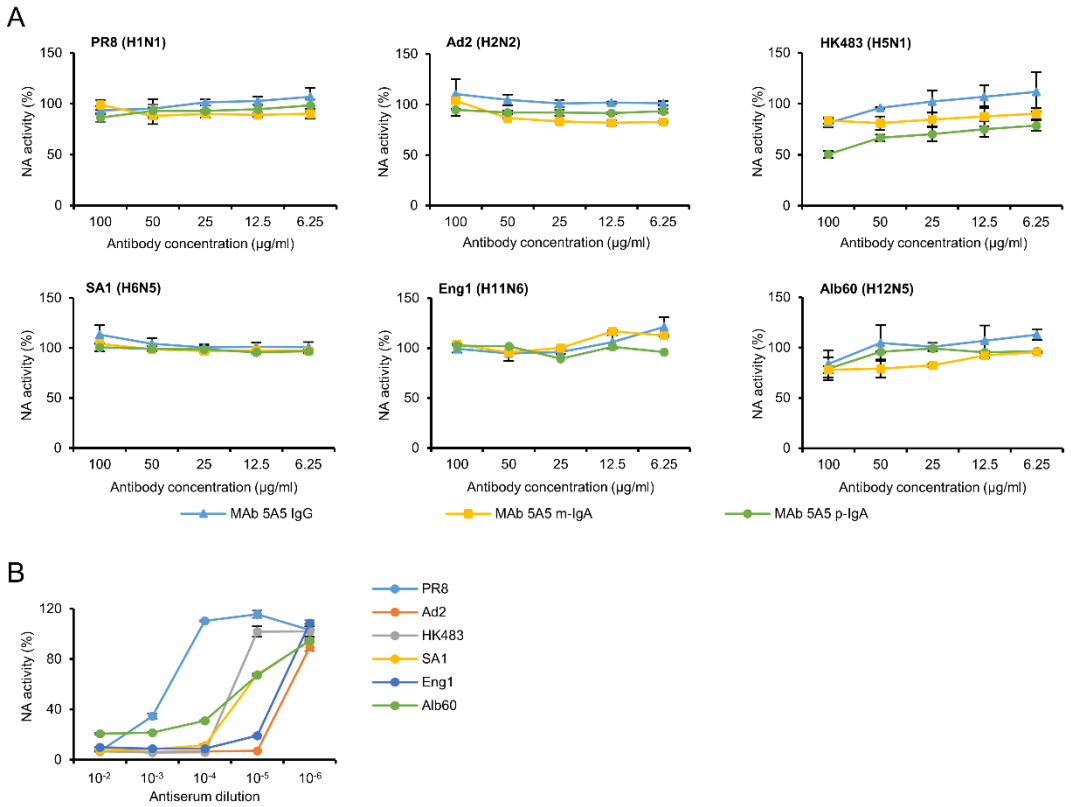

Figure 8 NI activity of MAb 5A5 antibodies

Two-fold serial dilutions of MAb 5A5 IgG, m-IgA, and p-IgA (6.25–100 μg/ml) (A), and ten-fold serial dilutions of positive control antisera (10^2 to 10^6-fold dilution) (B) were mixed with the respective IAV strains, followed by ELLA as described in Materials and Methods. Polyclonal chicken antisera against A/duck/Hokkaido/Vac-1/04 (H5N1), A/Singapore/1/1957 (H2N2), A/mallard/Astrakhan/263/1982 (H14N5), and Eng1 (H11N6) were used as positive control for N1, N2, N5, and N6. Means and standard deviations of NA activity were calculated from triplicate wells. Relative NA activity values to each control sample (i.e., viruses incubated without MAbs) are shown.

Reduction in plaque size by MAb 5A5

Since some antibodies having budding inhibition activity are known to reduce plaque sizes of IAVs (25, 83), the ability to inhibit plaque formation among MAbs 5A5 IgG, m-IgA, and p-IgA was compared. MDCK cells infected with the IAVs were incubated with three different forms of 5A5 and B12 MAbs, and plaque sizes were measured (Fig. 9). the plaque sizes of PR8, HK483, SA1, Eng1, and Alb60 were found to be significantly reduced in the presence of p-IgA, and that m-IgA also significantly reduced the plaque sizes of HK483, SA1, and Alb60, whereas MAb 5A5 IgG showed no significant reduction (Fig. 9). Furthermore, as expected, MAb 5A5 p-IgA showed higher ability to reduce plaque size than m-IgA against some of the IAV strains (PR8, SA1 and Eng1). Plaque size reduction was not observed with the control antibody, MAb B12. These results were consistent with the ability to reduce viral particle release from infected cells estimated by Western blotting and real-time RT-PCR analyses (Figs. 5 and 6).

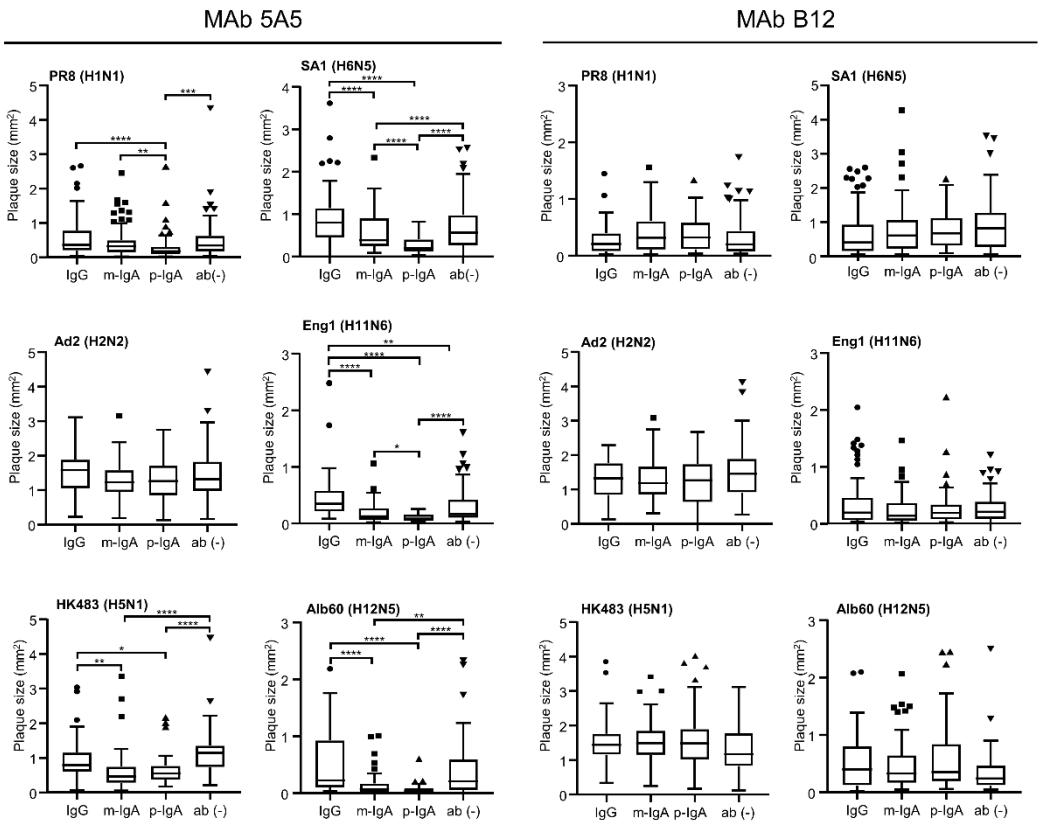

Figure 9 Reduced plaque size in the presence of 5A5 MAbs

MDCK cells were infected with IAVs and incubated with or without 5A5 or B12 MAbs (10 μg/ml). Plaques were stained as described in Materials and Methods (A) and plaque sizes were measured for each well (B). Each box with a horizontal black line represents the interquartile range (IQR) and the median. The marks represent outlying plots located over 1.5 × IQR from the upper quartile. Whiskers extend from the highest and lowest values within a fence. Asterisks indicate significant differences (*$p < 0.05$, **$p < 0.01$, ***$p < 0.001$, ****$p < 0.0001$) determined using one-way ANOVA followed by Tukey's multiple comparison tests.

Discussion

It was reported that intranasal, but not subcutaneous immunization, of mice induced heterosubtypic immunity against multiple IAV HA subtypes, most likely owing to HA-specific nonneutralizing p-IgA antibodies (67, 75). It is also known that nonneutralizing antibodies are generally produced upon immunization/vaccination and that neutralizing activity is not the only indicator for protective antibodies against IAV infection (24, 32, 41, 68, 81). Thus, the present study aimed at providing direct evidence for the potential role of such nonneutralizing antibodies in cross-protective immunity against IAVs, focusing on the IgA function during the viral egress from infected cells (42). Using anti-HA nonneutralizing MAbs (5A5 IgG, m-IgA, and p-IgA) recognizing a single epitope involved in inter-subtypic cross-reactivity, their inhibitory effects on virus particle release and plaque formation were compared *in vitro*.

MAb 5A5 IgA was revealed to inhibit virus particle release of multiple IAV strains of different HA subtypes more efficiently than IgG. The plaque sizes of the tested IAVs were accordingly reduced more significantly by MAb 5A5 IgA than by IgG (Fig. 9). Consistent with previous studies showing that p-IgA antibodies have more potential to neutralize IAVs than IgG (42) and that trimeric/tetrameric secretory IgA has stronger antiviral activity against IAVs than IgG and m-IgA (58, 64, 65), the present study indicated that p-IgA had enhanced ability to inhibit the release of IAV particles compared to IgG and m-IgA (Figs. 5–7). Although MAb 5A5 IgG, m-IgA, and p-IgA showed binding to Ad2 HA (Figs. 2 and 3A), they had limited effects on inhibiting virus particle release and plaque formation (Figs. 5, 6 and 9), suggesting that MAb 5A5 might bind to Ad2 HA with a slightly different affinity from the other five IAV strains tested in this study. Further studies are needed to investigate whether the antiviral activity of ch5A5 is limited against other virus strains of H2 subtype or not.

Since HAs are abundantly expressed on IAV-infected cells (46), MAb 5A5 is thought to bind to cell surface HAs and to tether the progeny virus particles newly produced by infected cells at the cell surface. Importantly, increased numbers of virus particles deposited on the cell surface were observed in the presence of MAb 5A5 p-IgA compared to the presence of IgG and m-IgA (Fig. 7), which is consistent with a previous study showing that neutralizing IgA antibodies accumulated virus particles more efficiently than IgG (42). However, interestingly, there was no remarkable difference among MAb 5A5 IgG, m-IgA, and p-IgA in the binding activity (i.e., avidity) to the viruses (Fig. 4). Because of the multiplicity of antigen binding sites in a single p-IgA molecule and the flexibility of the constant heavy chains of IgA antibodies resulting in higher affinity to the epitope (74), it is assumed that p-IgA has an advantage in the ability

to tether the virus particles at the cell surface. Since NA inhibitors (e.g., oseltamivir, zanamivir, and peramivir) have well-known protective efficacy against IAVs by inhibiting the virus budding process (28, 77, 78), broadly reactive anti-HA IgA antibodies that inhibit viral release from infected cells may contribute to cross-protective immunity against IAVs of multiple HA subtypes even if they do not have "classical" neutralizing activity. It is known that intranasal immunization of live attenuated influenza vaccine provides broad cross-protective immunity in animal models, most likely due to the induction of nasal IgA antibodies (21, 22). However, detailed mechanisms how IgA antibodies contribute to the cross-protection remain unknown (76). The present study suggests that cross-reactive nonneutralizing p-IgA induced by the intranasal vaccination may contribute to the protection. However, further studies are required to provide direct evidence of the importance of such IgA antibodies for cross-protective immunity *in vivo*.

In this study, MAb 5A5 was found to bind to the HA globular head region (Fig. 3). Some antibodies that inhibit virus release are known to bind to the HA globular head or stem region (42, 81, 82). Since MAb 5A5 has broad reactivities against multiple HA subtypes, I assume that its epitope is located in a highly conserved region among HA subtypes. Although it is difficult to determine the epitopes of nonneutralizing antibodies like MAb 5A5 by obtaining amino acid sequences of escape mutants, identification of such epitopes on IAV HAs may provide profound understanding of the regions that are important for inhibition of virus release from infected cells and some other antibody functions (e.g., antibody-dependent cellular cytotoxicity).

p-IgA antibodies are transferred intracellularly to the apical membrane by transcytosis and some IgA antibodies are known to inhibit viral protein functions intracellularly (10, 38, 84). Interestingly, IgA antibodies that do not have "classical" neutralizing activity effectively inhibit rotavirus and measles virus replication via this mechanism, which is called intracellular neutralization (10, 84). It has also been shown that anti-HA IgA, but not IgG, interacted with newly produced intracellular HA proteins in IAV-infected cells, thereby reducing viral titers (37). Nonneutralizing HA-specific IgA antibodies, therefore, may also have the ability to disturb the function or maturation of HA in infected cells. A recent study has demonstrated that intracellular neutralization against IAVs actually occurs in cells collected from patients' nasopharyngeal aspirates (30). Further studies are needed to confirm whether nonneutralizing cross-reactive anti-HA IgA antibodies contribute to the intracellular neutralization.

Summary

IgA antibodies on mucosal surfaces are known to play an important role in protection from IAV infection and are believed to be more potent than IgG for cross-protective immunity against IAVs of multiple HA subtypes. However, in general, neutralizing antibodies specific to HA are principally HA subtype-specific. Here I focus on nonneutralizing but broadly cross-reactive HA-specific IgA antibodies. Recombinant IgG, m-IgA, and p-IgA antibodies were generated based on the sequence of a mouse anti-HA MAb 5A5 that had no neutralizing activity but showed broad binding capacity to multiple HA subtypes. While confirming that there was no neutralizing activity of the recombinant MAbs against IAV strains A/Puerto Rico/8/1934 (H1N1), A/Adachi/2/1957 (H2N2), A/Hong Kong/483/1997 (H5N1), A/shearwater/ South Australia/1/1972 (H6N5), A/duck/England/1/1956 (H11N6), and A/duck/Alberta/60/1976 (H12N5), I found that p-IgA, but not m-IgA and IgG, significantly reduced budding and release of most of the viruses from infected cells. Electron microscopy demonstrated that p-IgA deposited newly produced virus particles on the surfaces of infected cells, most likely due to tethering of virus particles. Furthermore, p-IgA was found to show significantly higher activity to reduce plaque sizes of the viruses than IgG and m-IgA. These results suggest that nonneutralizing p-IgA reactive to multiple HA subtypes may play a role in inter-subtype cross-protective immunity against IAVs.

Chapter II:
Comparative analyses of the antiviral activities of IgG and IgA antibodies to influenza A virus matrix 2 protein

Introduction

The IAV M2 protein is antigenically highly conserved irrespective of the IAV subtype. The M2 protein possesses ion channel activity and membrane scission activity, which are important for virus entry and egress, respectively (56). At virus budding sites, HA may initiate the budding event and thus colocalization of M2 and HA on the infected cell membrane is normally observed (6, 56). Although the M2 protein presents on the virus particle surface, its amount incorporated into each virion is low; approximately 16–67 M2 monomers for every 500 HA molecules (60, 83). However, since this protein is abundantly expressed on the virus-infected cell surface, the M2 protein is considered to be a promising target for antiviral drugs and universal IAV vaccines (1, 17). In fact, previous studies demonstrated that the M2e-based immunization protected mice from lethal challenge with IAVs with various HA subtypes (12, 15, 31).

In this chapter, I focus on antiviral activities of M2e-specific antibodies. Previous studies have shown that M2e-specific mouse MAb, rM2ss23 IgG, is a nonneutralizing antibody, but inhibits plaque formation of IAVs mostly likely due to disturbing normal architecture of budding zone (35, 44) and similarly, another M2e-specific MAb 14C2, which is also a nonneutralizing antibody, is able to limit the growth of IAV *in vitro* (83). These studies suggest that anti-M2 antibodies have the potential to inhibit virus budding from infected cells and may contribute to cross-protective immunity against IAVs. I hypothesized that p-IgA antibodies might have a greater ability to restrict the virus budding process than IgG. Using the amino acid sequence of the rM2ss23 variable region, I constructed mouse-human chimeric rMss23 (ch-rM2ss23) IgA and IgG, which were assumed to recognize the same epitope and compared their antiviral activities *in vitro*.

Materials and Methods

Cells and viruses

MDCK cells were maintained in MEM (Sigma-Aldrich, St. Louis, MO, USA) supplemented with 10% bovine serum (Gibco, Waltham, MA, USA), 100 U/ml penicillin, and 0.1 mg/ml streptomycin (Gibco, Waltham, MA, USA). HEK 293T cells were maintained in DMEM (Sigma-Aldrich, St. Louis, MO, USA) supplemented with 10% FBS (Gibco, Waltham, MA, USA), 100 U/ml penicillin, and 0.1 mg/ml streptomycin (Gibco, Waltham, MA, USA). Expi 293F cells were maintained in Expi293 Expression Medium (Thermo Fisher Scientific, Waltham, MA, USA) as described in the manufacturer's instructions. After inoculation with IAVs, MDCK cells were cultured in 0.3% BSA/MEM with 5 μg/ml trypsin (Gibco, Waltham, MA, USA). MDCK were maintained at 37°C in 5% CO_2. Expi 293F cells were maintained at 37°C in 8% CO_2 with an orbital shaker at 125 rpm. IAV strains, Ad2 and A/Aichi/2/1968 (H3N2) (Aichi), were propagated in MDCK cells and stored at −80°C until use. Infectious titers were determined as PFU with MDCK cells. The use of infectious materials was approved by the Committee for Safety Management of Pathogens, CZC, HU (10[07]).

5'-RACE-PCR and sequencing

Total RNA was extracted from the hybridoma cells producing rM2ss23 IgG (44) using an RNeasy kit (Qiagen, Hilden, Germany) and reverse transcribed with a SMARTer RACE 5'/3' kit (Clontech, Shiga, Japan) using 5' RACE CDS primer A (Clontech, Shiga, Japan). The VH and VL genes encoding the variable region were amplified by PCR using SeqAmp DNA polymerase (Takara, Shiga, Japan) as described in the manufacturer's instructions. The amplified VH and VL genes were cloned into pCR-Blunt II-TOPO (Invitrogen, Carlsbad, CA, USA), and subjected to nucleotide sequencing using a version 3.1 BigDye Terminator sequencing kit (Applied Biosystems, Foster City, CA, USA) and Applied Biosystems 3130xl Genetic Analyzer (Applied Biosystems, Foster City, CA, USA).

Expression and purification of IgG and IgA antibodies

The VH and VL genes of rM2ss23 were amplified with restriction enzyme sites and ligated into α1H, γ1HC, and κLC vectors (38). Expi 293F cells were cotransfected with γ1HC- and κLC-expressing plasmids using an Expifectamine 293 Transfection kit (Gibco, Waltham, MA, USA) to express the human-mouse ch-rM2ss23 IgG antibody. For expressing ch-rM2ss23 IgA antibodies, Expi 293F cells were cotransfected with α1H-, κLC-, J chain-, and SC-expressing plasmids. ch-rM2ss23 IgG and IgA antibodies were

purified from Expi 293F cell supernatants by using UNOsphere SUPrA (BioRad, Hercules, CA, USA) and CaptureSelect IgA (Invitrogen, Carlsbad, CA, USA), respectively. IgA antibodies were subjected to GFC using a Superose 6 10/300 GL column (GE Healthcare, Little Chalfont, UK) with an AKTA avant 25 chromatography system (GE Healthcare, Little Chalfont, UK). Fractions were collected in PBS at a flow rate of 0.5 ml/min and analyzed by BN-PAGE using NativePAGE 4–16% Bis-Tris Protein Gels (Invitrogen, Carlsbad, CA, USA) with NativeMark (Invitrogen, Carlsbad, CA, USA), a molecular weight standard. Considering the results of BN-PAGE, the fractions were separated into three antibody subsets: m-IgA, dimeric IgA (d-IgA), and trimeric/tetrameric (or quadrimeric) IgA (t/q-IgA). Fractions for each IgA antibody subset were pooled and concentrated using Amicon Ultra 30K (Merck Millipore, Darmstadt, Germany). Negative control IgG and IgA antibodies (MAb B12) were generated as described previously (58). All antibodies were stored at −80°C until use. The use of recombinant antibodies was approved by Hokkaido University Safety Committee for Genetic Recombination Experiments (21[4]).

Expression of recombinant M2

Recombinant M2 proteins as antigens for ELISA were prepared as reported previously (41). Briefly, HEK 293T cells transfected with the protein expression vector pCAGGS (48) encoding recombinant M2 genes derived from Ad2 and Aichi using TransIT-LT1 (Mirus) were subjected to membrane protein extraction using a eukaryotic membrane protein extraction reagent kit (Thermo Fisher Scientific, Waltham, MA, USA). The extracted membrane proteins were diluted 1000-fold with PBS and used as antigens for ELISA. The use of recombinant antibodies was approved by Hokkaido University Safety Committee for Genetic Recombination Experiments (21[4]).

ELISA

ELISA plates (Nunc Maxisorp, Invitrogen, Carlsbad, CA, USA) were coated with the prepared M2 antigens and blocked with 3% skim milk (Becton Dickinson, Franklin Lakes, NJ, USA) in PBS. ch-rM2ss23 IgG, m-IgA, d-IgA, and t/q-IgA antibodies diluted in 1% skim milk in PBST were plated in triplicate, and the bound antibodies were detected using HRP-conjugated goat anti-human IgG (H+L) (109-001-003, Jackson Immuno Research, West Grove, PA, USA) or HRP-conjugated goat anti-human IgA (H+L) (ab97215, Abcam, Cambridge, UK). The reaction was visualized by adding TMB (Sigma-Aldrich, St. Louis, MO, USA) and absorbance at 450 nm was measured.

SPR assay

SPR assay was performed using Biacore 3000 (GE Healthcare, Little Chalfont, UK) as described previously (58). Briefly, the synthetic Aichi M2e peptide with a C-terminal His-tag (Cosmo Bio, Tokyo, Japan) was immobilized on the surface of Sensor Chip NTA (GE Healthcare, Little Chalfont, UK) by using an NTA reagent kit (GE Healthcare, Little Chalfont, UK). After Aichi M2e immobilization (10 μg/ml), the molecular interactions of M2e with ch-rM2ss23 IgG, m-IgA, d-IgA, and t/q-IgA (10 μg/ml) were analyzed.

Neutralization assay

Appropriately diluted IAVs (100 PFU) were incubated with serial dilutions of ch-rM2ss23 antibodies (0.01–100 μg/ml) and then inoculated into MDCK cells. Anti-HA MAb S139/1, which neutralizes both Ad2 and Aichi (41, 42), was used as a positive control antibody. After incubation with the virus-MAb mixture, the cells were washed with PBS and overlaid with 0.3% BSA/MEM containing 1.2% Avicel RC 591 (FMC BioPolymer, Philadelphia, PA, USA) (36) and 5 μg/ml trypsin. After 20-hour incubation, the cells were fixed with methanol and blocked with 1% BSA in PBS. Plaques were stained with MAb S139/1, HRP-conjugated goat anti-mouse IgG (H+L) (115-035-062, Jackson Immuno Research, West Grove, PA, USA), and a 3,3'-diaminobenzidine substrate (Wako, Osaka, Japan).

Plaque size reduction assay

MDCK cells seeded on 12-well plates (Corning, Corning, NY, USA) were infected with appropriately diluted IAVs (50–100 PFU) and overlaid with 0.3% BSA/MEM containing 5 μg/ml trypsin, 0.8% agarose S (Wako, Osaka, Japan), and IgG and IgA forms of ch-rM2ss23 or the control antibody (MAb B12). After incubation with or without MAbs for two days at 35°C, plaques were visualized with immunostaining using the same methods as described above for the neutralizing assay. Plaque images on each well were scanned and the sizes of at least 30 plaques for each condition were measured using ImageJ analysis software.

Sample collection of cell lysates and supernatants of infected cells

MDCK cells seeded on 12-well plates (Corning, Corning, NY, USA) were incubated with IAVs at m.o.i. of 2.0 for one hour, and then washed with PBS. Subsequently, the infected cells were incubated in the presence or absence of IgG and IgA forms of ch-rM2ss23 or MAb B12. After 8-hour incubation, the supernatant was

centrifuged and collected into new tubes. Laemmli sample buffer (BioRad, Hercules, CA, USA) containing 2-mercaptoethanol was added to the cells and lysates were collected for Western blotting.

Western blotting

Cell lysates and supernatants mixed with the sample buffer were incubated at 95°C for 10 and 5 minutes, respectively. After 12% SDS-PAGE, separated proteins were transferred onto PVDF membranes (Merck Millipore, Darmstadt, Germany). The PVDF membranes were soaked with 3% skim milk (Becton Dickinson, Franklin Lakes, NJ, USA) in PBS and washed with PBST. Each membrane was incubated with a mouse anti-M1 MAb (APH 6-23-1-6) (45) and a mouse anti-beta actin antibody (ab6276, Abcam, Cambridge, UK) as primary antibodies and subsequently with HRP-conjugated goat anti-mouse IgG (H+L) (115-035-062, Jackson Immuno Research, West Grove, PA, USA) as a secondary antibody. These antibodies were diluted with PBST containing 1.5% skim milk. The bound antibodies were visualized with Immobilon Western (Merck Millipore, Darmstadt, Germany). The amount of the viral M1 protein was semi-quantified based on the band intensity using Amersham Imager 600 (GE Healthcare, Little Chalfont, UK).

RT-PCR

Viral RNA was extracted from the cell supernatant using a QIAmp Viral RNA Mini Kit (Qiagen, Hilden, Germany) and subjected to real-time RT-PCR-based IAV gene detection using one-step SYBR prime script RT-PCR kit II (Takara, Shiga, Japan). Primer sets specific for conserved regions of the IAV NP gene (NP 972F [CAAGAGTCAGCTGGTGTGGA] and NP 1160R [GCCCAGTACCTGCTTCTCAG]) were used. Quantification of the NP gene was performed using a standard curve generated by threshold cycle values obtained from 10-fold serial dilutions (covering 10^2 to 10^6 copies) of the PR8 NP gene inserted into the pHH21 vector (47). All samples were tested in triplicate. Average copy numbers of the viral genome in the supernatant of IAV-infected cells incubated without any MAb were set to 100%.

TEM

TEM was performed as described previously (42, 49). Briefly, MDCK cells infected with Aichi at m.o.i. 1.0–2.0 were cultured with or without ch-rM2ss23 IgG, m-IgA, d-IgA, or t/q-IgA (1 μg/ml) for 8 hours and fixed with 2.5% glutaraldehyde in 0.1 M cacodylate buffer (pH 7.4). The fixed cells were postfixed with 2% osmium tetroxide and dehydrated with series of ethanol gradients followed by propylene oxide, embedded in

Epon 812 Resin mixture (TAAB Laboratories Equipment Ltd., Berks, UK), and polymerized. Ultrathin sections (50 nm) were stained with uranyl acetate and lead citrate and examined with a JEM-1210 (JEOL, Tokyo, Japan) electron microscope at 80 kV.

Statistical analysis

Data (band intensity, RNA copy number, and plaque size) were analyzed using GraphPad Prism version 8 for Windows (GraphPad Software, San Diego, CA, USA). One-way ANOVA followed by Tukey's multiple comparison test was used to analyze each data set as indicated in the figure legends. The following statistical values and symbols are used throughout the manuscript; *$p < 0.05$, **$p < 0.01$, ***$p < 0.001$; ****$p < 0.0001$.

Results

Production of mouse-human chimeric rM2ss23 IgG and IgA antibodies

To compare the antiviral activities of the IgG and IgA anti-M2 antibodies, mouse-human chimeric IgG and IgA antibodies were generated based on the sequence of the rM2ss23 (44) variable region. The VH and VL genes of rM2ss23 were cloned into heavy and light chain expression plasmids for IgG and IgA and then Expi 293F cells were transfected with the constructed plasmids. To generate p-IgA antibodies, SC and J chain expression plasmids were cotransfected. After affinity purification of ch-rM2ss23 IgG and IgA from the supernatant, different forms of IgA antibodies were separated based on their molecular weights by GFC (Fig. 10A); fractions 1–4, 6–10, and 12–14 were pooled for t/q-IgA, d-IgA, and m-IgA, respectively. The purity and molecular weights of the purified antibodies were validated (Fig. 10B) and used for further experiments.

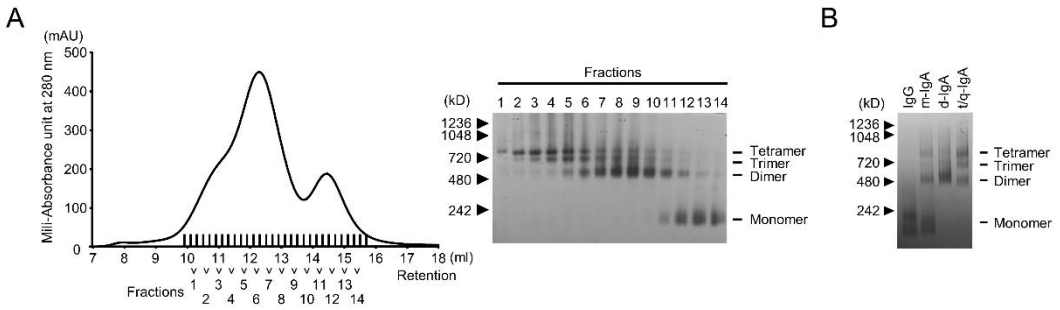

Figure 10 Purification of ch-rM2ss23 IgA. ch-rM2ss23 IgA antibodies were fractionated by GFC with a Superose 6 10/300 GL column

A chromatogram demonstrating absorbance at 280 nm (shown in milli-absorbance units [mAU]) reveals two major peaks (A, left panel). Fractions covering the two peaks were subjected to BN-PAGE (A, right panel). Equal amounts (5 μg) of purified ch-rM2ss23 IgG, m-IgA, d-IgA, and t/q-IgA were used for BN-PAGE (B).

Binding activities of ch-rM2ss23 IgG and IgA

The binding activities of ch-rM2ss23 IgG and IgA antibodies were examined using recombinant M2 proteins of Ad2 and Aichi in ELISA. It was revealed that the reactivities of p-IgA antibodies (i.e., d-IgA and t/q-IgA) to both M2 proteins tested were higher than that of m-IgA and that IgG showed lower OD values than any of the IgA forms (Fig. 11A). However, since different secondary antibodies (HRP-labeled anti-IgG or anti-IgA antibodies) were used in ELISA, I assumed that it is not reasonable to directly compare binding capacities between IgG and IgA antibodies in this assay. To further assess the binding activities of the antibodies, the binding dynamics of ch-rM2ss23 IgG, m-IgA, d-IgA, and t/q-IgA were investigated by SPR analysis to quantify the avidity of each ch-rM2ss23 to Aichi M2e (Fig. 11B). The SPR response of ch-rM2ss23 IgG was found to be decreased slightly faster than the IgA antibodies, indicating that the IgG had only a slightly higher dissociation rate (i.e., weaker binding) than IgA antibodies. Of note, there was no remarkable difference in dissociation rates among m-IgA, d-IgA, and t/q-IgA. These data suggest that the isotype conversion from IgG1 to the IgA1 backbone had only limited effects on the affinity/avidity of ch-rM2ss23. The increased OD values of d-IgA and t/q-IgA in ELISA might have been due to their polymeric forms giving multiple IgA monomers that provided more binding sites for the secondary antibody. Taken together, these data suggested that the antibody avidity of ch-rM2ss23 was minimally affected by IgA polymerization.

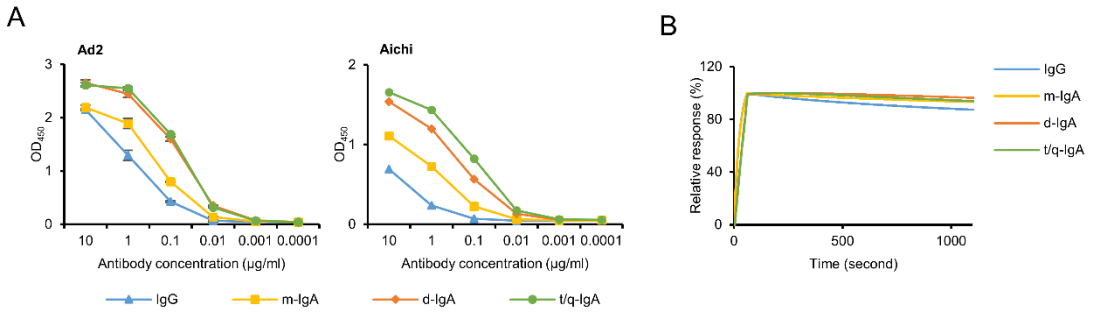

Figure 11 Comparison of binding to M2 antigens among ch-rM2ss23 antibodies

Reactivities of IgG, m-IgA, d-IgA, and t/q-IgA (0.0001–10 μg/ml) to recombinant M2 proteins of Ad2 and Aichi were measured in ELISA (A). Binding dynamics of ch-rM2ss23 IgG, m-IgA, d-IgA, and t/q-IgA to the synthetic Aichi M2e peptide (B). Sensorgrams were adjusted (x=0, y=0: baseline, y=100: binding) to allow comparisons between different antibody forms in terms of the dissociation rate.

Reduction in plaque size in the presence of ch-rM2ss23 IgG and IgA antibodies

It was confirmed that ch-rM2ss23 IgG and IgA antibodies did not possess neutralizing activity against either of two IAVs tested (Fig. 12). These results were consistent with a study showing that the mouse rM2ss23 IgG antibody bound to Aichi M2 but did not show neutralizing activity (44).

Previous studies have indicated that anti-M2 antibodies, including rM2ss23, inhibit plaque formation of IAVs when the antibody is present in the overlay medium (44, 83). Therefore, the ability to reduce plaque sizes among ch-rM2ss23 IgG, m-IgA, d-IgA, and t/q-IgA antibodies was compared (Fig. 13). MDCK cells infected with the IAVs were incubated with four different forms of ch-rM2ss23 and three different forms of the negative control MAb B12 (i.e., IgG, m-IgA, and p-IgA), and plaque sizes were measured. It was revealed that the plaque sizes of Ad2 and Aichi were significantly reduced in the presence of ch-rM2ss23 IgA antibodies, whereas IgG showed minimal reduction at these concentrations. The inhibitory effect of ch-rM2ss23 IgG was similar to that of original mouse rM2ss23 (44). Plaque size reduction was not observed with control MAb B12 antibodies. These results indicated that the ch-rM2ss23 t/q-IgA antibody possessed higher antiviral activity against Ad2 and Aichi than the IgG or m-IgA antibody. The mechanism of the antiviral activity of ch-rM2ss23 t/q-IgA antibodies was further analyzed in the following experiments.

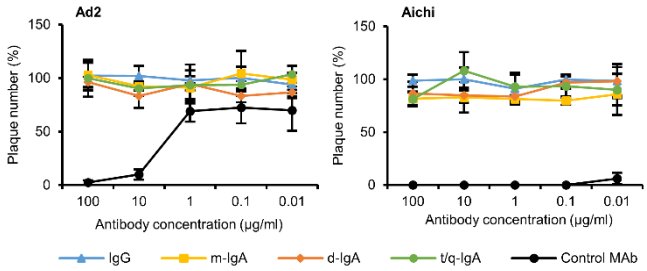

Figure 12 Neutralization tests of ch-rM2ss23 antibodies

Serial dilutions of ch-rM2ss23 IgG, m-IgA, d-IgA, and t/q-IgA and positive control neutralizing MAb (0.01–100 μg/ml) were mixed with each IAV strain, followed by plaque assays. Means and standard deviations of plaque numbers were calculated from three individual experiments. Relative plaque numbers to each control sample (i.e. cells incubated without MAbs) are shown.

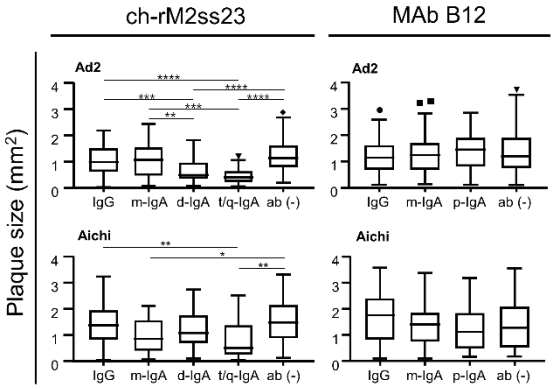

Figure 13 Reduced plaque sizes of IAVs in the presence of ch-rM2ss23 IgA antibodies
MDCK cells were infected with IAVs and incubated with or without MAb B12 and ch-rM2ss23 antibodies. Ad2- and Aichi-infected cells were incubated with MAbs at 10 μg/ml and 0.5 μg/ml, respectively. Plaques were stained as described in Materials and Methods (A) and plaque sizes were measured for each well (B). Each box with a horizontal black line represents the IQR and the median. The marks represent outlying plots located over 1.5 × IQR from the upper quartile. Whiskers extend from the highest and lowest values within a fence. Asterisks indicate significant differences (*$p < 0.05$, **$p < 0.01$, ***$p < 0.001$, ****$p < 0.0001$) determined using one-way ANOVA followed by Tukey's multiple comparison test.

Reduction of viral particles released from IAV-infected cells in the presence of ch-rM2ss23 IgG and IgA antibodies

Since nonneutralizing antibodies often have the potential to interfere with the virus release process (41, 59), inhibitory effects of ch-rM2ss23 on virus release from MDCK cells infected with IAVs were examined (Fig. 14A). The amounts of M1 proteins were significantly lower in the supernatants of ch-rM2ss23-treated cells than in those of MAb-untreated cells. It was noted that t/q-IgA decreased the amount of M1 more significantly than IgG and/or m-IgA. There was no remarkable inhibitory effect with control MAb B12 IgG, m-IgA, and p-IgA. Similar expression levels of the M1 protein of these two IAV strains were observed in cell lysates among the MAb treatments, indicating that viral protein synthesis was not affected by the treatment with the antibodies (Fig. 14B).

To further analyze the amounts of virus particles released from the IAV-infected cells, viral RNA (NP gene) in the supernatants was quantified by real-time RT-PCR assays. The copy numbers of the NP gene of Ad2 and Aichi were confirmed to be significantly decreased in the supernatants of the cells incubated with ch-rM2ss23 t/q-IgA compared to those of the cells incubated with IgG or m-IgA (Fig. 15). Taken together, these results indicated that ch-rM2ss23 t/q-IgA had higher antiviral activity than IgG and m-IgA to reduce the amounts of IAV particles released into cell culture supernatants.

A previous study reported that unusual aggregation and accumulation of virus particles were found on the IAV-infected cells cultured in the presence of MAbs which inhibited the IAV release from infected cells (42). To investigate whether ch-rM2ss23 antibodies aggregate virus particles on the surface of IAV-infected cells, Aichi-infected MDCK cells incubated with ch-rM2ss23 IgG, m-IgA, d-IgA, or t/q-IgA were observed by TEM. Small numbers of virus particles in low proximity on the infected cells were found regardless of the presence of ch-rM2ss23 IgG and IgA antibodies as well as MAb-untreated cells (Fig. 16).

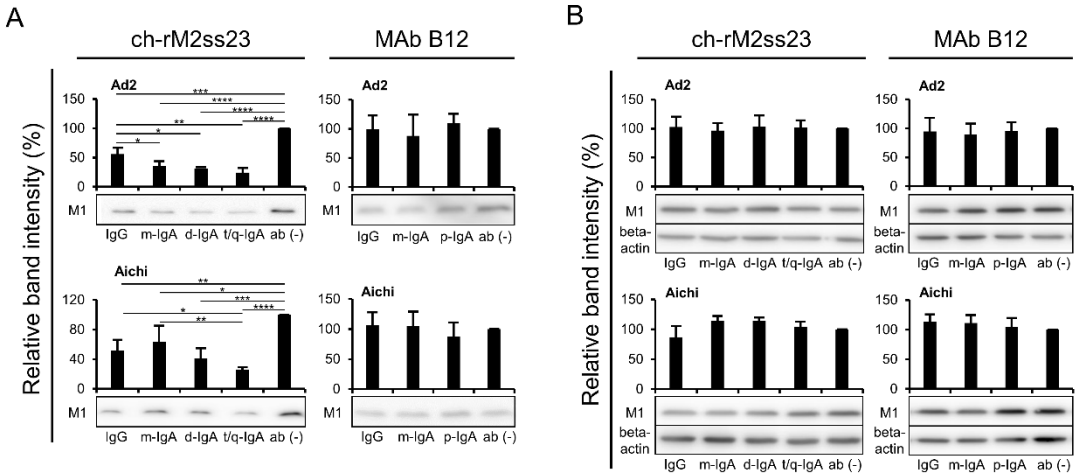

Figure 14 Detection of the viral protein in supernatants and lysates of IAV-infected cells

MDCK cells plated in 12-well plates were infected with IAVs at m.o.i. 2.0 and incubated with or without MAbs B12 and ch-rM2ss23 for 8 hours at 35°C. The cells infected with Ad2 and Aichi were incubated with or without the MAbs at 10 μg/ml and 1 μg/ml, respectively. The M1 protein in supernatants (A) and cell lysates (B) was detected in Western blotting. Beta-actin was also stained for cell lysate samples. Band intensities relative to each control sample (i.e., cells incubated without MAbs) are shown. Each experiment was performed three times and averages and standard deviations are shown. Asterisks indicate significant differences (*$p < 0.05$, **$p < 0.01$, ***$p < 0.001$, ****$p < 0.0001$) found using one-way ANOVA followed by Tukey's multiple comparison test.

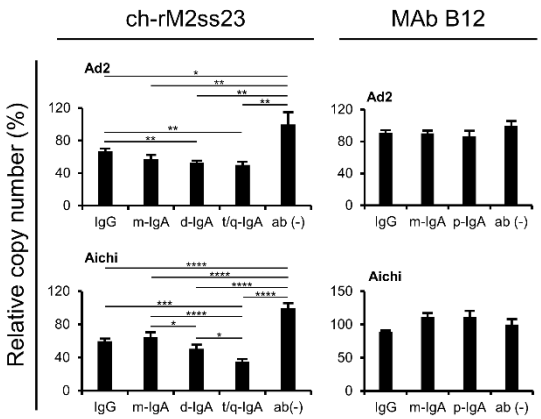

Figure 15 Detection of the viral RNA genome in the supernatants of IAV-infected cells

MDCK cells were infected with IAVs at m.o.i. 2.0 and incubated with or without MAb B12 and ch-rM2ss23 antibodies. The cells infected with Ad2 and Aichi were incubated with or without the MAbs at 10 μg/ml and 1 μg/ml, respectively. The viral RNA genome was detected by real-time RT-PCR. The average copy number of the viral genome in the supernatant of IAV-infected cells incubated without MAbs was set to 100%. Each experiment was performed three times and averages and standard deviations are shown. Asterisks indicate significant differences (*$p < 0.05$, **$p < 0.01$, ***$p < 0.001$, ****$p < 0.0001$) determined using one-way ANOVA followed by Tukey's multiple comparison test.

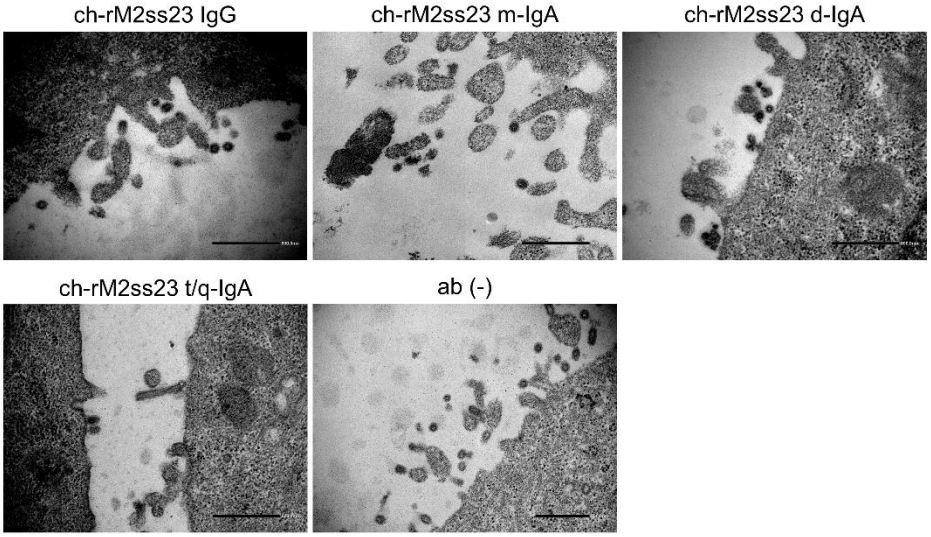

Figure 16 Electron microscopy of virus particles on the surface of Aichi-infected cells
MDCK cells were infected with Aichi at m.o.i. of 2.0 and incubated for eight hours with or without ch-rM2ss23 IgG, m-IgA, d-IgA, and t/q-IgA. Scale bars represent 500 nm.

Discussion

Compared to the IAV envelope glycoproteins (i.e., HA and NA), M2 protein is antigenically well conserved among all IAVs that caused past pandemics in humans, and it does not have a significant rate of antigenic drift (23, 57). Although the M2 protein works as a proton-selective channel and mediates the release of viral RNA into the cytosol (55, 70), anti-M2 antibodies that inhibit virus entry into cells have rarely been reported. It is also known that the M2 protein is important for budding of newly produced IAV particles from infected cells (6, 39, 60). I, therefore, focused on the potential role of anti-M2 IgA antibodies in cross-protective immunity against IAVs. In the present study, the inhibitory effects of anti-M2 nonneutralizing MAbs (ch-rM2ss23 IgG, m-IgA, d-IgA, and t/q-IgA) on the virus budding and plaque formation processes of IAVs *in vitro* were compared and ch-rM2ss23 t/q-IgA antibodies were revealed to show higher antiviral activity than IgG antibodies.

It has been shown that IgA antibodies often possess higher affinity to a single epitope than IgG due to altered flexibility of their constant heavy chains (8). Accordingly, previous studies demonstrated that p-IgA antibodies showed higher antiviral activity than IgG (42, 69). In the present study, the dissociation rates of ch-rM2ss23 m-IgA, d-IgA, and t/q-IgA were slightly lower than that of IgG, which might contribute to stronger budding inhibition of IgA antibodies (Fig. 11B). Interestingly, however, although there was no remarkable difference in the antibody avidity among ch-rM2ss23 m-IgA, d-IgA, and t/q-IgA, t/q-IgA had relatively higher antiviral activity. This is most likely due to the multiplicity of antigen binding sites in a single t/q-IgA molecule.

A previous study found aggregation and accumulation of virus particles on the IAV-infected cells cultured in the presence of anti-HA MAbs that inhibited the IAV release from the cells (42). Since the M2 protein is abundantly expressed on the surface of IAV-infected cells as well as the HA protein (83), I assumed that ch-rM2ss23 antibodies likely bound to the M2 protein on the cell surface and tethered progeny virus particles newly produced from infected cells, as was shown with anti-HA antibodies (42). However, virus particles were not accumulated or agglutinated in the presence of ch-rM2ss23 IgG and IgA antibodies (Fig. 16), suggesting that ch-rM2ss23 might inhibit IAV release into cell supernatants via a mechanism different from that of anti-HA MAbs reported previously (42). In the normal architecture of viral budding sites, viral integral membrane proteins (i.e. HA, NA, and M2), NP, and M1 proteins interact with each other (34). Previous reports suggest that colocalization of HA and M2 is necessary for IAVs to effectively egress from the cells (56, 70). Recently, the antiviral activity of rM2ss23 IgG was revealed to be derived from disturbance of M2-HA colocalization on the IAV-infected cell surface

(35). Thus, it might be possible that the distribution of M2 proteins on the infected cells was strongly altered by ch-rM2ss23 IgA antibodies and the disrupted M2 localization interfered with the interaction with HA, leading to the reduction of newly produced virus particles from infected cells.

p-IgA antibodies are transferred intracellularly via pIgR to the apical membrane of epithelial cells and some of those antibodies are known to inhibit viral protein functions during the transcytosis (10, 38, 84). Indeed, it was shown that anti-HA IgA, but not IgG, interacted with HA proteins newly synthesized in the IAV-infected cells, and subsequently reduced the viral growth (37). Anti-M2 IgA antibodies, therefore, may have the potential to bind to M2 molecules in the IAV-infected cell and readily interfere with the function of M2 intracellularly, which may result in inhibiting virus particle formation. Further studies are needed to confirm whether anti-M2 IgA antibodies contribute to intracellular neutralization.

The present study suggests that M2-specific t/q-IgA antibodies exhibit enhanced antiviral activity compared to IgG. Further studies are needed to confirm the contribution of M2-specific IgA antibodies to protection from IAV infection *in vivo*.

Summary

The IAV M2 protein is an antigenically conserved viral envelope protein that plays an important role in virus budding together with HA protein. An M2-specific mouse MAb rM2ss23, which binds to the M2e protein, has been shown to be a nonneutralizing antibody but inhibits plaque formation of IAV strains. In this study, ch-rM2ss23 IgG and IgA antibodies having the same variable region were generated and their antiviral activities were compared. Using gel chromatography, ch-rM2ss23 IgA were divided into three antibody subsets: m-IgA, d-IgA, and t/q-IgA. t/q-IgA was found to have a significantly higher capacity to reduce the plaque size of IAVs than IgG and m-IgA, most likely due to the decreased number of progeny virus particles produced from infected cells. Since the accumulation of virus particles on the surface of IAV-infected cells was not observed by TEM, ch-rM2ss23 antibodies would inhibit virus budding process but not virus release. These results suggest that anti-M2 t/q-IgA restricts IAV budding more efficiently than IgG and suggest a role of anti-M2 IgA in cross-protective immunity to IAVs.

Conclusion

Mucosal immunity represented by p-IgA antibodies plays important roles in protection from IAV infection. Furthermore, virus-specific p-IgA antibodies are thought to contribute to cross-protective immunity against multiple IAV subtypes. However, it is also known that the vast majority of IAV neutralizing antibodies are subtype-specific. In the present study, I investigated the potential roles of nonneutralizing IgA antibodies in cross-protective immunity against IAVs, focusing on HA- and M2-specific antibodies that are cross-reactive to multiple HA subtypes.

In chapter I, I investigated antiviral mechanisms of HA-specific IgA using a nonneutralizing but broadly cross-reactive HA-specific antibody, MAb 5A5, and found that p-IgA, but not m-IgA and IgG, significantly reduced budding and release of the viruses with various HA subtypes from infected cells. Furthermore, p-IgA showed significantly higher activity to reduce plaque sizes of the viruses than IgG and m-IgA. TEM demonstrated that p-IgA deposited newly produced virus particles on the surfaces of infected cells. These results suggest the ability of HA-specific nonneutralizing IgA to inhibit IAV budding and release, which is likely due to tethering of virus particles.

In chapter II, I compared antiviral activities of IgG and IgA using an M2-specific cross-reactive MAb, rM2ss23. I found that t/q-IgA had a significantly higher capacity to reduce the plaque size of IAVs than IgG and m-IgA. Furthermore, t/q-IgA reduced virus particles in the supernatant of IAV-infected cells. Since rM2ss23 IgG is known to inhibit M2-HA colocalization and resulted in plaque size reduction, t/q-IgA might alter M2-HA colocalization stronger than IgG and m-IgA. These results indicate that anti-M2 t/q-IgA restricts IAV budding more efficiently than IgG and suggest a role of anti-M2 IgA in cross-protective immunity to IAVs.

The present study highlights potential roles of nonneutralizing p-IgA antibodies in inter-subtypic cross-protective immunity against IAVs. The results support the idea that mucosal vaccination may provide heterosubtypic immunity to IAVs by inducing nonneutralizing but cross-reactive p-IgA antibodies that inhibit the release of viruses from infected cells. Further analyses on the *in vivo* function of p-IgA will provide new insights into strategies to induce a broad spectrum of protective immunity against multiple IAV HA subtypes, including the viruses with pandemic potential.

Acknowledgments

I would like to express my sincere gratitude to my supervisor Prof. Ayato Takada (Division of Global Epidemiology, Research Center for Zoonosis Control [CZC], Hokkaido University [HU]) for the continuous support of my research, for his patience, motivation, and immense knowledge. His guidance helped me in all the time of research and writing of this thesis.

I sincerely appreciate the invaluable suggestions and advice from Prof. Yasuhiko Suzuki (Division of Bioresourses, CZC, HU), Prof. Hirofumi Sawa (Division of Molecular Pathobiology, CZC, HU), and Prof. Yoshihiro Sakoda (Laboratory of Microbiology, Faculty of Veterinary Medicine, HU). Each of you has given advice that has helped me to refine my Ph.D. and expand my research skills.

I would like to specially thank Associate Prof. Manabu Igarashi, Assistant Prof. Reiko Yoshida, Assistant Prof. Rashid Manzoor, and Assistant Prof. Masahiro Kajihara (Division of Global Epidemiology, CZC, HU) for their technical and intellectual support. I would like to thank to all the members of the Division of Global Epidemiology for their kind and heartfelt support.

I am also grateful to thank Prof. Hideaki Higashi (Division of Infection and Immunity, CZC, HU), Associate Prof. Osamu Ichii (Laboratory of Anatomy, Faculty of Veterinary Medicine, HU), and Lecturer Dr. Michihito Sasaki (Division of Molecular Pathobiology, Research CZC, HU) for their technical support and insightful comments.

I would like to thank Dr. Shinji Saito (Influenza Virus Research Center, National Institute of Infectious Diseases) and Dr. Tadaki Suzuki (Department of Pathology, National Institute of Infectious Diseases) for their technical support and their provision of important materials (e.g., antibody expression plasmids)

I am grateful to the coordinator at the Program for Leading Graduate Schools, HU, Prof. Motohiro Horiuchi (Laboratory of Veterinary Hygiene, Faculty of Veterinary Medicine, HU), and the members of the Leading Program Office for their help with my Ph.D. coursework.

This work was supported by the Research Fellowship for Young Scientists from the Japan Society for the Promotion of Science.

Abstract in Japanese

A 型インフルエンザウイルス (IAV) は、ヘマグルチニン (HA)、ノイラミニダーゼ (NA) およびマトリックス 2 (M2) タンパク質を粒子表面にもつ。HA および NA は抗原性の違いからそれぞれ複数の亜型に分類される。一方、M2 タンパク質は、HA および NA 亜型に関わらずウイルス株間で抗原性が高く保存されている。HA は IAV の標的細胞表面への結合および細胞侵入を担っており、NA は感染細胞から IAV が放出される際に重要な機能を持っている。M2 タンパク質は、イオンチャネルとして IAV の細胞侵入に働くだけでなく、感染細胞外への出芽過程にも重要な役割を担うことが分かっている。

HA はウイルスの細胞侵入に必須であるため、中和抗体の標的である。しかし、大部分の中和抗体は HA 亜型特異的であり、複数の亜型のウイルス株に対して中和活性を示す抗 HA 抗体は限られている。一方、粘膜面に分泌される IgA 抗体は IgG 抗体よりも亜型間交差反応性が高く、IAV に対する感染防御に重要であると考えられている。しかし、複数の亜型の IAV に対して IgA 抗体が抗ウイルス作用を示す機序は未だ不明である。本学位論文では、非中和抗体に着目し、幅広い亜型のウイルスに交差反応性を示す HA および M2 特異的モノクローナル抗体を用いて、様々なウイルス株に対する抗ウイルス活性を IgG 抗体と IgA 抗体との間で比較解析した。

第一章では、HA 特異的抗体による抗ウイルス活性を調べた。複数の異なる亜型の HA に結合能を有するマウスモノクローナル抗体 5A5 の可変領域の遺伝子配列を基に、ヒト IgG および IgA 抗体発現プラスミドを用いて、同じエピトープを持つヒト―マウスキメラ IgG および IgA 抗体を作出した。IgA 抗体は多量体を形成するため、ゲル濾過クロマトグラフィーにより単量体 IgA および多量体 IgA 抗体の 2 つに分画した。各抗体存在下で、IAV A/Puerto Rico/8/1934 (H1N1) (PR8)、A/Adachi/2/1957 (H2N2) (Ad2)、A/Hong Kong/483/1997 (H5N1) (HK483)、A/shearwater/ South Australia/1/1972 (H6N5) (SA1)、A/duck/England/1/1956 (H11N6) (Eng1) および A/duck/Alberta/60/1976 (H12N5) (Alb60) 株を感染させた培養細胞の上清中に含まれるウイルスタンパク質およびウイルス遺伝子を定量した。その結果、IgG および単量体 IgA 抗体存在下と比較して、多量体 IgA 抗体存在下では PR8、HK483、SA1、Eng1 および Alb60 株に感染させた細胞上清中のウイルスタンパク質および遺伝子量が有意に減少する事が分かった。IgA 抗体存在下では、感染細胞表面にウイルス粒子が集積している像が電子顕微鏡でみられ、単量体 IgA 抗体と比較して多量体 IgA 抗体でより強く集積していた。さらに、ウイルス増殖の指標であるプラーク形成能に及ぼす影響を抗体間で比較したところ、多量体 IgA 抗体存在下では PR8、HK483、SA1、Eng1 および Alb60 のプラークサイズが顕著に減少した。また、作出した IgG および IgA 抗体は IAV の NA 活

性を阻害しないことを確認した。以上の結果から、多量体 IgA 抗体は、非中和抗体であっても、ウイルス粒子および感染細胞表面上に存在する HA に結合し架橋することでウイルス粒子が細胞から遊離する過程を阻害する事が示唆された。

第二章では、M2 特異的抗体による抗ウイルス活性を IgG および IgA 抗体間で比較解析した。先行研究から、M2 タンパク質に結合するマウスモノクローナル抗体 rM2ss23 (IgG)は、Ad2 および A/Aichi/2/1968 (H3N2) (Aichi) に結合し、細胞侵入阻害による中和活性は示さないものの、これらのウイルスのプラークサイズを小さくさせることが分かっていた。そこで、第一章同様に rM2ss23 と同じエピトープを持つヒト―マウスキメラ IgG および IgA 抗体を作出し、出芽阻害活性を比較解析した。IgA 抗体は多量体を形成するため、ゲル濾過クロマトグラフィーにより単量体 IgA、二量体 IgA、三・四量体 IgA の 3 つに分画した。プラーク形成能に及ぼす影響をこれらの抗体間で比較したところ、三・四量体 IgA 抗体存在下では、Ad2 および Aichi のプラークサイズが IgG 抗体存在下と比較して有意に縮小した。また、感染細胞の上清中に含まれるウイルスタンパク質量およびウイルス遺伝子量は、三・四量体 IgA 抗体存在下で IgG および単量体 IgA と比較して有意に減少した。各抗体存在下における感染細胞を電子顕微鏡で観察したところ、ウイルス粒子が集積している像は見られなかった。以上のことから、M2 特異的 IgA 抗体は、ウイルスの出芽過程自体を効率よく阻害することで抗ウイルス活性を示す可能性が示唆された。

本研究により、IAV に対する非中和 IgA 抗体が抗ウイルス活性を発揮するメカニズムの一端が明らかになった。本研究の結果から、粘膜免疫の誘導によって産生される、複数の亜型の IAV に対して交差反応性を有する非中和 p-IgA 抗体は、IAV の出芽過程を阻害することで亜型間交差感染防御免疫に関与する可能性が示唆された。今後、p-IgA 抗体の生体内での機能を解析することによって、亜型に制限されない感染防御免疫の誘導法の開発につながると考えられる。そのようなワクチンが実現すれば、将来出現する新型インフルエンザウイルスにも効果が期待される。

References

1. **Adler-Moore, J. P., W. Ernst, H. Kim, N. Ward, S. M. Chiang, T. Do, and G. Fujii.** 2017. Monomeric M2e antigen in VesiVax((R)) liposomes stimulates protection against type a strains of influenza comparable to liposomes with multimeric forms of M2e. J Liposome Res **27:**210-220.
2. **Brandtzaeg, P.** 1974. Presence of J chain in human immunocytes containing various immunoglobulin classes. Nature **252:**418-420.
3. **Calder, L. J., S. Wasilewski, J. A. Berriman, and P. B. Rosenthal.** 2010. Structural organization of a filamentous influenza A virus. Pro Natl Acad Sci U S A. **107:**10685-10690.
4. **Cate, T. R., Y. Rayford, D. Nino, P. Winokur, R. Brady, R. Belshe, W. Chen, R. L. Atmar, and R. B. Couch.** 2010. A high dosage influenza vaccine induced significantly more neuraminidase antibody than standard vaccine among elderly subjects. Vaccine **28:**2076-2079.
5. **Caton, A. J., G. G. Brownlee, J. W. Yewdell, and W. Gerhard.** 1982. The antigenic structure of the influenza virus A/PR/8/34 hemagglutinin (H1 subtype). Cell **31:**417-427.
6. **Chen, B. J., G. P. Leser, D. Jackson, and R. A. Lamb.** 2008. The influenza virus M2 protein cytoplasmic tail interacts with the M1 protein and influences virus assembly at the site of virus budding. J Virol. **82:**10059-10070.
7. **Chen, Y. Q., L. Y. Lan, M. Huang, C. Henry, and P. C. Wilson.** 2019. Hemagglutinin Stalk-Reactive Antibodies Interfere with Influenza Virus Neuraminidase Activity by Steric Hindrance. J Virol. **93**.
8. **Chizhmakov, I. V., F. M. Geraghty, D. C. Ogden, A. Hayhurst, M. Antoniou, and A. J. Hay.** 1996. Selective proton permeability and pH regulation of the influenza virus M2 channel expressed in mouse erythroleukaemia cells. The J Physiol. **494 (Pt 2):**329-336.
9. **Cohen, M., X. Q. Zhang, H. P. Senaati, H. W. Chen, N. M. Varki, R. T. Schooley, and P. Gagneux.** 2013. Influenza A penetrates host mucus by cleaving sialic acids with neuraminidase. Virol J. **10:**321.
10. **Corthesy, B., Y. Benureau, C. Perrier, C. Fourgeux, N. Parez, H. Greenberg, and I. Schwartz-Cornil.** 2006. Rotavirus anti-VP6 secretory immunoglobulin A contributes to protection via intracellular neutralization but not via immune exclusion. J Virol. **80:**10692-10699.
11. **Corti, D., J. Voss, S. J. Gamblin, G. Codoni, A. Macagno, D. Jarrossay, S. G. Vachieri, D. Pinna, A. Minola, F. Vanzetta, C. Silacci, B. M. Fernandez-**

Rodriguez, G. Agatic, S. Bianchi, I. Giacchetto-Sasselli, L. Calder, F. Sallusto, P. Collins, L. F. Haire, N. Temperton, J. P. Langedijk, J. J. Skehel, and A. Lanzavecchia. 2011. A neutralizing antibody selected from plasma cells that binds to group 1 and group 2 influenza A hemagglutinins. Science **333:**850-856.

12. **Dabaghian, M., A. M. Latifi, M. Tebianian, H. NajmiNejad, and S. M. Ebrahimi.** 2018. Nasal vaccination with r4M2e.HSP70c antigen encapsulated into N-trimethyl chitosan (TMC) nanoparticulate systems: Preparation and immunogenicity in a mouse model. Vaccine **36:**2886-2895.
13. **Edinger, T. O., M. O. Pohl, and S. Stertz.** 2014. Entry of influenza A virus: host factors and antiviral targets. J Gen Virol. **95:**263-277.
14. **Ekiert, D. C., G. Bhabha, M. A. Elsliger, R. H. Friesen, M. Jongeneelen, M. Throsby, J. Goudsmit, and I. A. Wilson.** 2009. Antibody recognition of a highly conserved influenza virus epitope. Science **324:**246-251.
15. **Fan, J., X. Liang, M. S. Horton, H. C. Perry, M. P. Citron, G. J. Heidecker, T. M. Fu, J. Joyce, C. T. Przysiecki, P. M. Keller, V. M. Garsky, R. Ionescu, Y. Rippeon, L. Shi, M. A. Chastain, J. H. Condra, M. E. Davies, J. Liao, E. A. Emini, and J. W. Shiver.** 2004. Preclinical study of influenza virus A M2 peptide conjugate vaccines in mice, ferrets, and rhesus monkeys. Vaccine **22:**2993-3003.
16. **Fleury, D., B. Barrere, T. Bizebard, R. S. Daniels, J. J. Skehel, and M. Knossow.** 1999. A complex of influenza hemagglutinin with a neutralizing antibody that binds outside the virus receptor binding site. Nat Struct Biol. **6:**530-534.
17. **Gordon, N. A., K. L. McGuire, S. K. Wallentine, G. A. Mohl, J. D. Lynch, R. G. Harrison, and D. D. Busath.** 2017. Divalent copper complexes as influenza A M2 inhibitors. Antiviral Res. **147:**100-106.
18. **Gould, V. M. W., J. N. Francis, K. J. Anderson, B. Georges, A. V. Cope, and J. S. Tregoning.** 2017. Nasal IgA Provides Protection against Human Influenza Challenge in Volunteers with Low Serum Influenza Antibody Titre. Front Microbiol. **8:**900.
19. **Hai, R., F. Krammer, G. S. Tan, N. Pica, D. Eggink, J. Maamary, I. Margine, R. A. Albrecht, and P. Palese.** 2012. Influenza viruses expressing chimeric hemagglutinins: globular head and stalk domains derived from different subtypes. J Virol. **86:**5774-5781.
20. **Holsinger, L. J., M. A. Shaughnessy, A. Micko, L. H. Pinto, and R. A. Lamb.** 1995. Analysis of the posttranslational modifications of the influenza virus M2 protein. J Virol. **69:**1219-1225.

21. **Isakova-Sivak, I., V. Matyushenko, T. Kotomina, I. Kiseleva, E. Krutikova, S. Donina, A. Rekstin, N. Larionova, D. Mezhenskaya, K. Sivak, A. Muzhikyan, A. Katelnikova, and L. Rudenko.** 2019. Sequential Immunization with Universal Live Attenuated Influenza Vaccine Candidates Protects Ferrets against a High-Dose Heterologous Virus Challenge. Vaccines **7:**61.

22. **Ito, R., Y. A. Ozaki, T. Yoshikawa, H. Hasegawa, Y. Sato, Y. Suzuki, R. Inoue, T. Morishima, N. Kondo, T. Sata, T. Kurata, and S. Tamura.** 2003. Roles of anti-hemagglutinin IgA and IgG antibodies in different sites of the respiratory tract of vaccinated mice in preventing lethal influenza pneumonia. Vaccine **21:**2362-2371.

23. **Ito, T., O. T. Gorman, Y. Kawaoka, W. J. Bean, and R. G. Webster.** 1991. Evolutionary analysis of the influenza A virus M gene with comparison of the M1 and M2 proteins. J Virol. **65:**5491-5498.

24. **Jegaskanda, S., E. R. Job, M. Kramski, K. Laurie, G. Isitman, R. de Rose, W. R. Winnall, I. Stratov, A. G. Brooks, P. C. Reading, and S. J. Kent.** 2013. Cross-reactive influenza-specific antibody-dependent cellular cytotoxicity antibodies in the absence of neutralizing antibodies. J Immunol. **190:**1837-1848.

25. **Job, E. R., M. Schotsaert, L. I. Ibanez, A. Smet, T. Ysenbaert, K. Roose, M. Dai, C. A. M. de Haan, H. Kleanthous, T. U. Vogel, and X. Saelens.** 2018. Antibodies Directed toward Neuraminidase N1 Control Disease in a Mouse Model of Influenza. J Virol. **92:** e01584-17.

26. **Johansen, F. E., R. Braathen, and P. Brandtzaeg.** 2000. Role of J chain in secretory immunoglobulin formation. Scand J Immunol. **52:**240-248.

27. **Kida, H., L. E. Brown, and R. G. Webster.** 1982. Biological activity of monoclonal antibodies to operationally defined antigenic regions on the hemagglutinin molecule of A/Seal/Massachusetts/1/80 (H7N7) influenza virus. Virology **122:**38-47.

28. **Kim, C. U., W. Lew, M. A. Williams, H. Liu, L. Zhang, S. Swaminathan, N. Bischofberger, M. S. Chen, D. B. Mendel, C. Y. Tai, W. G. Laver, and R. C. Stevens.** 1997. Influenza neuraminidase inhibitors possessing a novel hydrophobic interaction in the enzyme active site: design, synthesis, and structural analysis of carbocyclic sialic acid analogues with potent anti-influenza activity. J Am Chem Soc. **119:**681-690.

29. **Klenk, H. D., R. Rott, M. Orlich, and J. Blodorn.** 1975. Activation of influenza A viruses by trypsin treatment. Virology **68:**426-439.

30. **Kok, T. W., M. Costabile, G. A. Tannock, and P. Li.** 2018. Colocalization of

intracellular specific IgA (icIgA) with influenza virus in patients' nasopharyngeal aspirate cells. J Virol Methods. **252:**8-14.

31. **Kolpe, A., B. Schepens, W. Fiers, and X. Saelens.** 2017. M2-based influenza vaccines: recent advances and clinical potential. Expert Rev Vaccines. **16:**123-136.
32. **Krammer, F., and P. Palese.** 2013. Influenza virus hemagglutinin stalk-based antibodies and vaccines. Curr Opin Virol. **3:**521-530.
33. **Lambre, C. R., H. Terzidis, A. Greffard, and R. G. Webster.** 1991. An enzyme-linked lectin assay for sialidase. Clin Chim Acta. **198:**183-193.
34. **Leser, G. P., and R. A. Lamb.** 2017. Lateral Organization of Influenza Virus Proteins in the Budozone Region of the Plasma Membrane. J Virol. **91:**e02104-16.
35. **Manzoor, R., Eguchi, N., Yoshida, R., Ozaki, H., Kondoh, T., Okuya, K., Miyamoto, H., and Takada, A.** 2020. A Novel Mechanism Underlying Antiviral Activity of an Influenza Virus M2-Specific Antibody. J Virol. **95**: e01277-20.
36. **Matrosovich, M., T. Matrosovich, W. Garten, and H. D. Klenk.** 2006. New low-viscosity overlay medium for viral plaque assays. Virol J. **3:**63.
37. **Mazanec, M. B., C. L. Coudret, and D. R. Fletcher.** 1995. Intracellular neutralization of influenza virus by immunoglobulin A anti-hemagglutinin monoclonal antibodies. J Virol. **69:**1339-1343.
38. **Mazanec, M. B., C. S. Kaetzel, M. E. Lamm, D. Fletcher, and J. G. Nedrud.** 1992. Intracellular neutralization of virus by immunoglobulin A antibodies. Pro Natl Acad Sci U S A. **89:**6901-6905.
39. **McCown, M. F., and A. Pekosz.** 2005. The influenza A virus M2 cytoplasmic tail is required for infectious virus production and efficient genome packaging. J Virol. **79:**3595-3605.
40. **Medina, R. A., and A. Garcia-Sastre.** 2011. Influenza A viruses: new research developments. Nat Rev Microbiol. **9:**590-603.
41. **Muramatsu, M., R. Yoshida, H. Miyamoto, D. Tomabechi, M. Kajihara, J. Maruyama, T. Kimura, R. Manzoor, K. Ito, and A. Takada.** 2013. Heterosubtypic antiviral activity of hemagglutinin-specific antibodies induced by intranasal immunization with inactivated influenza viruses in mice. PLoS One. **8:**e71534.
42. **Muramatsu, M., R. Yoshida, A. Yokoyama, H. Miyamoto, M. Kajihara, J. Maruyama, N. Nao, R. Manzoor, and A. Takada.** 2014. Comparison of antiviral activity between IgA and IgG specific to influenza virus hemagglutinin: increased

potential of IgA for heterosubtypic immunity. PLoS One. **9:**e85582.

43. **Murphy, B. R., and M. L. Clements.** 1989. The systemic and mucosal immune response of humans to influenza A virus. Curr Top Microbiol Immunol. **146:**107-116.
44. **Muto, N. A., R. Yoshida, T. Suzuki, S. Kobayashi, H. Ozaki, D. Fujikura, R. Manzoor, M. Muramatsu, A. Takada, T. Kimura, and H. Sawa.** 2012. Inhibitory effects of an M2-specific monoclonal antibody on different strains of influenza A virus. Jpn J Vet Res. **60:**71-83.
45. **Nao, N., M. Kajihara, R. Manzoor, J. Maruyama, R. Yoshida, M. Muramatsu, H. Miyamoto, M. Igarashi, N. Eguchi, M. Sato, T. Kondoh, M. Okamatsu, Y. Sakoda, H. Kida, and A. Takada.** 2015. A Single Amino Acid in the M1 Protein Responsible for the Different Pathogenic Potentials of H5N1 Highly Pathogenic Avian Influenza Virus Strains. PLoS One. **10:**e0137989.
46. **Nayak, D. P., E. K. Hui, and S. Barman.** 2004. Assembly and budding of influenza virus. Virus Res. **106:**147-165.
47. **Neumann, G., T. Watanabe, H. Ito, S. Watanabe, H. Goto, P. Gao, M. Hughes, D. R. Perez, R. Donis, E. Hoffmann, G. Hobom, and Y. Kawaoka.** 1999. Generation of influenza A viruses entirely from cloned cDNAs. Pro Natl Acad Sci U S A. **96:**9345-9350.
48. **Niwa, H., K. Yamamura, and J. Miyazaki.** 1991. Efficient selection for high-expression transfectants with a novel eukaryotic vector. Gene **108:**193-199.
49. **Noda, T., H. Sagara, E. Suzuki, A. Takada, H. Kida, and Y. Kawaoka.** 2002. Ebola virus VP40 drives the formation of virus-like filamentous particles along with GP. J Virol. **76:**4855-4865.
50. **Norderhaug, I. N., F. E. Johansen, H. Schjerven, and P. Brandtzaeg.** 1999. Regulation of the formation and external transport of secretory immunoglobulins. Crit Rev Immunol. **19:**481-508.
51. **Ohuchi, M., N. Asaoka, T. Sakai, and R. Ohuchi.** 2006. Roles of neuraminidase in the initial stage of influenza virus infection. Microbes Infect. **8:**1287-1293.
52. **Okada, J., N. Ohshima, R. Kubota-Koketsu, Y. Iba, S. Ota, W. Takase, T. Yoshikawa, T. Ishikawa, Y. Asano, Y. Okuno, and Y. Kurosawa.** 2011. Localization of epitopes recognized by monoclonal antibodies that neutralized the H3N2 influenza viruses in man. J Gen Virol. **92:**326-335.
53. **Okuno, Y., K. Matsumoto, Y. Isegawa, and S. Ueda.** 1994. Protection against the mouse-adapted A/FM/1/47 strain of influenza A virus in mice by a monoclonal antibody with cross-neutralizing activity among H1 and H2 strains. J Virol.

68:517-520.

54. **Palese, P., K. Tobita, M. Ueda, and R. W. Compans.** 1974. Characterization of temperature sensitive influenza virus mutants defective in neuraminidase. Virology **61:**397-410.
55. **Pinto, L. H., L. J. Holsinger, and R. A. Lamb.** 1992. Influenza virus M2 protein has ion channel activity. Cell **69:**517-528.
56. **Rossman, J. S., X. Jing, G. P. Leser, and R. A. Lamb.** 2010. Influenza virus M2 protein mediates ESCRT-independent membrane scission. Cell **142:**902-913.
57. **Saelens, X.** 2019. The Role of Matrix Protein 2 Ectodomain in the Development of Universal Influenza Vaccines. J Infect Dis. **219:**S68-S74.
58. **Saito, S., K. Sano, T. Suzuki, A. Ainai, Y. Taga, T. Ueno, K. Tabata, K. Saito, Y. Wada, Y. Ohara, H. Takeyama, T. Odagiri, T. Kageyama, K. Ogawa-Goto, P. Multihartina, V. Setiawaty, K. N. A. Pangesti, and H. Hasegawa.** 2019. IgA tetramerization improves target breadth but not peak potency of functionality of anti-influenza virus broadly neutralizing antibody. PLoS Pathog. **15:**e1007427.
59. **Schneemann, A., J. A. Speir, G. S. Tan, R. Khayat, D. C. Ekiert, Y. Matsuoka, and I. A. Wilson.** 2012. A virus-like particle that elicits cross-reactive antibodies to the conserved stem of influenza virus hemagglutinin. J Virol. **86:**11686-11697.
60. **Schroeder, C., H. Heider, E. Moncke-Buchner, and T. I. Lin.** 2005. The influenza virus ion channel and maturation cofactor M2 is a cholesterol-binding protein. Eur Biophys J. **34:**52-66.
61. **Skehel, J. J., and D. C. Wiley.** 2000. Receptor binding and membrane fusion in virus entry: the influenza hemagglutinin. Annu Rev Biochem. **69:**531-569.
62. **Steel, J., A. C. Lowen, T. T. Wang, M. Yondola, Q. Gao, K. Haye, A. Garcia-Sastre, and P. Palese.** 2010. Influenza virus vaccine based on the conserved hemagglutinin stalk domain. mBio **1:** e00018-10.
63. **Steinhauer, D. A.** 1999. Role of hemagglutinin cleavage for the pathogenicity of influenza virus. Virology **258:**1-20.
64. **Suzuki, T., A. Ainai, and H. Hasegawa.** 2017. Functional and structural characteristics of secretory IgA antibodies elicited by mucosal vaccines against influenza virus. Vaccine **35:**5297-5302.
65. **Suzuki, T., A. Kawaguchi, A. Ainai, S. Tamura, R. Ito, P. Multihartina, V. Setiawaty, K. N. Pangesti, T. Odagiri, M. Tashiro, and H. Hasegawa.** 2015. Relationship of the quaternary structure of human secretory IgA to neutralization of influenza virus. Pro Natl Acad Sci U S A. **112:**7809-7814.
66. **Takada, A., N. Kuboki, K. Okazaki, A. Ninomiya, H. Tanaka, H. Ozaki, S.**

Itamura, H. Nishimura, M. Enami, M. Tashiro, K. F. Shortridge, and H. Kida. 1999. Avirulent Avian influenza virus as a vaccine strain against a potential human pandemic. J Virol. **73:**8303-8307.

67. **Takada, A., S. Matsushita, A. Ninomiya, Y. Kawaoka, and H. Kida.** 2003. Intranasal immunization with formalin-inactivated virus vaccine induces a broad spectrum of heterosubtypic immunity against influenza A virus infection in mice. Vaccine **21:**3212-3218.
68. **Terajima, M., J. Cruz, M. D. Co, J. H. Lee, K. Kaur, J. Wrammert, P. C. Wilson, and F. A. Ennis.** 2011. Complement-dependent lysis of influenza a virus-infected cells by broadly cross-reactive human monoclonal antibodies. J Virol. **85:**13463-13467.
69. **Terauchi, Y., K. Sano, A. Ainai, S. Saito, Y. Taga, K. Ogawa-Goto, S. I. Tamura, T. Odagiri, M. Tashiro, M. Fujieda, T. Suzuki, and H. Hasegawa.** 2018. IgA polymerization contributes to efficient virus neutralization on human upper respiratory mucosa after intranasal inactivated influenza vaccine administration. Hum Vaccin Immunother. **14:**1351-1361.
70. **Thaa, B., A. Herrmann, and M. Veit.** 2010. Intrinsic cytoskeleton-dependent clustering of influenza virus M2 protein with hemagglutinin assessed by FLIM-FRET. J Virol. **84:**12445-12449.
71. **Tiller, T., E. Meffre, S. Yurasov, M. Tsuiji, M. C. Nussenzweig, and H. Wardemann.** 2008. Efficient generation of monoclonal antibodies from single human B cells by single cell RT-PCR and expression vector cloning. J Immunol Methods. **329:**112-124.
72. **Tong, S., Y. Li, P. Rivailler, C. Conrardy, D. A. Castillo, L. M. Chen, S. Recuenco, J. A. Ellison, C. T. Davis, I. A. York, A. S. Turmelle, D. Moran, S. Rogers, M. Shi, Y. Tao, M. R. Weil, K. Tang, L. A. Rowe, S. Sammons, X. Xu, M. Frace, K. A. Lindblade, N. J. Cox, L. J. Anderson, C. E. Rupprecht, and R. O. Donis.** 2012. A distinct lineage of influenza A virus from bats. Pro Natl Acad Sci U S A. **109:**4269-4274.
73. **Tsuchiya, E., K. Sugawara, S. Hongo, Y. Matsuzaki, Y. Muraki, Z. N. Li, and K. Nakamura.** 2001. Antigenic structure of the haemagglutinin of human influenza A/H2N2 virus. J Gen Virol. **82:**2475-2484.
74. **Tudor, D., H. Yu, J. Maupetit, A. S. Drillet, T. Bouceba, I. Schwartz-Cornil, L. Lopalco, P. Tuffery, and M. Bomsel.** 2012. Isotype modulates epitope specificity, affinity, and antiviral activities of anti-HIV-1 human broadly neutralizing 2F5 antibody. Pro Natl Acad Sci U S A. **109:**12680-12685.

75. **Tumpey, T. M., M. Renshaw, J. D. Clements, and J. M. Katz.** 2001. Mucosal delivery of inactivated influenza vaccine induces B-cell-dependent heterosubtypic cross-protection against lethal influenza A H5N1 virus infection. J Virol. **75:**5141-5150.

76. **Turner, P. J., A. F. Abdulla, M. E. Cole, R. R. Javan, V. Gould, M. E. O'Driscoll, J. Southern, M. Zambon, E. Miller, N. J. Andrews, K. Hoschler, and J. S. Tregoning.** 2020. Differences in nasal immunoglobulin A responses to influenza vaccine strains after live attenuated influenza vaccine (LAIV) immunization in children. Clin Exp Immunol. **199:**109-118.

77. **Varghese, J. N., J. L. McKimm-Breschkin, J. B. Caldwell, A. A. Kortt, and P. M. Colman.** 1992. The structure of the complex between influenza virus neuraminidase and sialic acid, the viral receptor. Proteins **14:**327-332.

78. **von Itzstein, M., W. Y. Wu, G. B. Kok, M. S. Pegg, J. C. Dyason, B. Jin, T. Van Phan, M. L. Smythe, H. F. White, S. W. Oliver, and et al.** 1993. Rational design of potent sialidase-based inhibitors of influenza virus replication. Nature **363:**418-423.

79. **Westgeest, K. B., T. M. Bestebroer, M. I. Spronken, J. Gao, L. Couzens, A. D. Osterhaus, M. Eichelberger, R. A. Fouchier, and M. de Graaf.** 2015. Optimization of an enzyme-linked lectin assay suitable for rapid antigenic characterization of the neuraminidase of human influenza A(H3N2) viruses. J Virol Methods. **217:**55-63.

80. **Wu, Y., Y. Wu, B. Tefsen, Y. Shi, and G. F. Gao.** 2014. Bat-derived influenza-like viruses H17N10 and H18N11. Trends Microbiol. **22:**183-191.

81. **Yamayoshi, S., R. Uraki, M. Ito, M. Kiso, S. Nakatsu, A. Yasuhara, K. Oishi, T. Sasaki, K. Ikuta, and Y. Kawaoka.** 2017. A Broadly Reactive Human Anti-hemagglutinin Stem Monoclonal Antibody That Inhibits Influenza A Virus Particle Release. EBioMedicine. **17:**182-191.

82. **Yoshida, R., M. Igarashi, H. Ozaki, N. Kishida, D. Tomabechi, H. Kida, K. Ito, and A. Takada.** 2009. Cross-protective potential of a novel monoclonal antibody directed against antigenic site B of the hemagglutinin of influenza A viruses. PLoS Pathog. **5:**e1000350.

83. **Zebedee, S. L., and R. A. Lamb.** 1988. Influenza A virus M2 protein: monoclonal antibody restriction of virus growth and detection of M2 in virions. J Virol. **62:**2762-2772.

84. **Zhou, D., Y. Zhang, Q. Li, Y. Chen, B. He, J. Yang, H. Tu, L. Lei, and H. Yan.** 2011. Matrix protein-specific IgA antibody inhibits measles virus replication by

intracellular neutralization. J Virol. **85:**11090-11097.